ACS OMEGA

http://pubs.acs.org/journal/acsodf

Article

Facile One-Pot Synthesis of Functionalized Quinoline-Fused Fluorescent Dihydro/Spiro-quinazolinone Derivatives

Kevin George, Pavithra Elavarasan, Shanmugam Ponnusamy,* and Kannadasan Sathananthan*

Cite This: *ACS Omega* 2022, 7, 20605−20618

Read Online

ACCESS | Metrics & More | Article Recommendations | Supporting Information

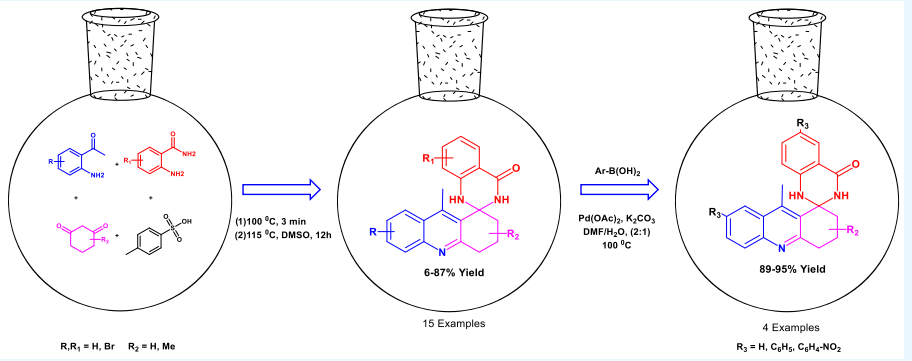

ABSTRACT: A facile and efficient method has been developed for the synthesis of quinoline-fused fluorescent dihydro/spiro-quinazolinones. A plausible mechanism involving an acid-mediated enaminone intermediate is provided. The reaction proceeded using *p*-toluene sulfonic acid as a green promoter. The methodology was successful in synthesizing various quinoline-appended spiro-quinazolinones **4a−o**. The synthetic utility of compounds **4a−o** was demonstrated by synthesizing compounds **6a−d** via Suzuki coupling as a key reaction. Significantly, the $\pi-\pi^*$ electronic transition of compounds **4c** and **4k** showed a blue shift. The molar extinction coefficient (ε), Stoke's shift ($\Delta\bar{u}$), and quantum yield $(\Phi^f)_c$ were calculated for these derivatives (**4c** and **4k**).

INTRODUCTION

The chemistry of quinoline scaffolds is well documented. Owing to their biological properties, it leads to great interest among medicinal chemists in the development of drug candidates. Various classical methods such as Skraup, Doebner-von Miller, Friedländer, Pfitzinger, Conrad-Limpach, and Combes synthesis are known for a quinoline ring system.[1] Later, due to the importance of the quinoline backbone, a number of new methods have been developed by employing both transition metals and metal-free conditions such as CuCN, $LiCl_3$, $RuCl_3$,[2] $Yb(OTf)_3$,[3] tungsten vinylidene complex,[4] BF_3OEt_2,[5,6] benzotriazoleiminium salts, etc.[7] Notably, cabozantinib, and bosutinib are a few FDA-approved marketed anticancer drugs containing a quinoline moiety[8] and a quinazolinone skeleton present in many drugs and natural products such as bouchardatine, rutaecarpine, etc. (Figure 1).[9] Owing to the diverse range of pharmacological activities, various methods have been developed using copper,[10,11] iridium,[12] manganese,[13] silver,[14] vanadium,[15] cyanuric chloride,[16] cationic Amberlyst-15 resin,[17] clays,[18] *p*-TSA,[19] starch sulfate,[20] and TFA[21] for the synthesis of quinazolinone derivatives. Indeed, the nitrogen-containing heterocyclic compounds play a significant role in biological activities such as chorismate mutase inhibitors, IRAP inhibitors, etc. (Figure 1).[22]

Recently, molecular hybridization has been developed as a tool in the development of hybrid analogues with enhanced potency by combining two or more pharmacophores of bioactive scaffolds. The molecular hybridization of various biologically active pharmacophores resulted in lead compounds with multifaceted biological activity wherein specific as well as multiple targets were involved.[23] Thus, we were interested to develop molecular hybridization having quinoline and quinazolinone cores. A few reports are available for the synthesis of quinoline-fused quinazolines. One such example is Luotonin A (Figure 1), a pyrroloquinazolinoquinoline alkaloid extracted from the Chinese medicinal plant *Peganum nigellastrum*. Nevertheless, although the mechanism is unknown, Luotonin A is cytotoxic toward the murine leukemia P-388 cell line (IC_{50} 1.8 μg/mL).[24]

To minimize waste and reaction time, "step-economic" and "pot-economic" syntheses have emerged as efficient and

Received: February 2, 2022
Accepted: May 27, 2022
Published: June 9, 2022

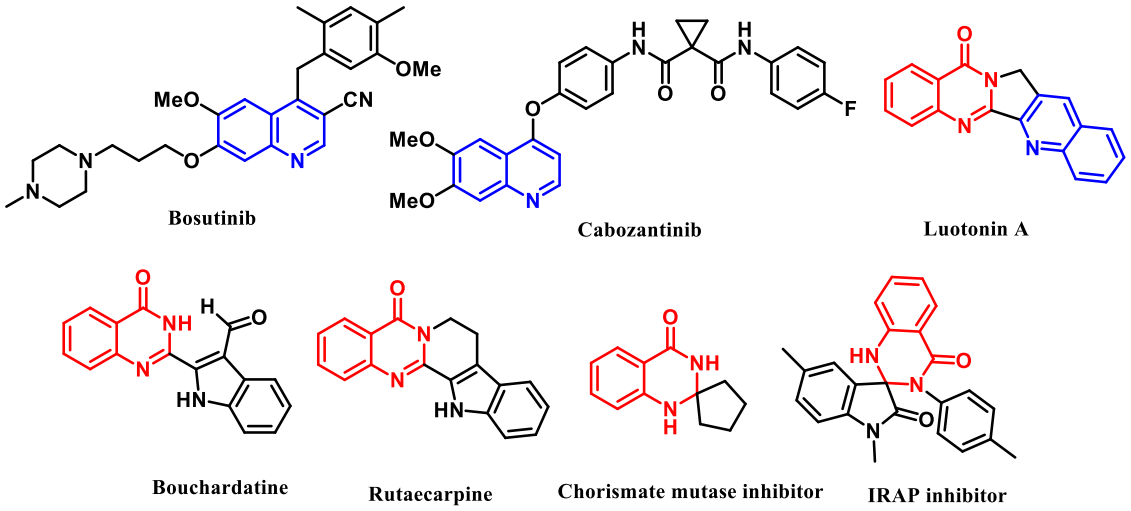

Figure 1. Biologically active molecules having quinoline and quinazolinone cores.

Scheme 1. Synthesis of Quinoline-Fused Quinazolinone

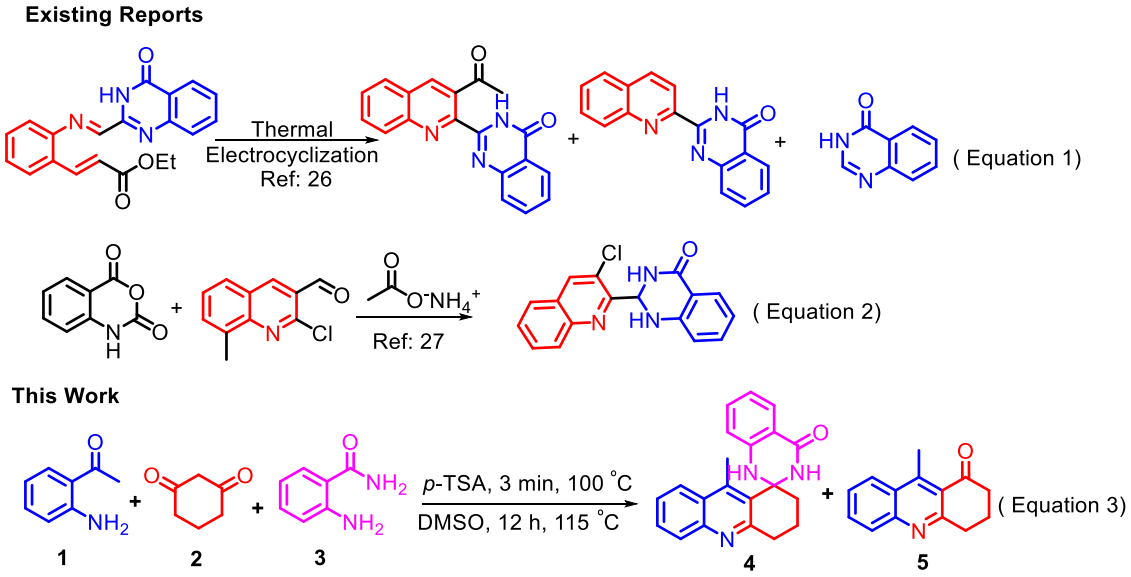

sustainable reaction protocols. Since the beginning, one-pot reactions have grown in two directions, namely, multiple orthogonal, irreversible steps are combined, while in the second case, multiple reversible steps are coupled to one irreversible step using an enzymatic catalyst.[25] To the best of our knowledge, the synthesis of quinoline-appended quinazolinone in a one-pot manner is reported via thermal electrocyclization of aldimine[26] (Scheme 1, equation 1) and the synthesis of 2-hetero-substituted 2,3-dihydroquinazolin-4(3*H*)-ones is carried out using Mont. K10 clay as a catalyst[27] (Scheme 1, equation 2). Thus, we have developed a novel one-pot protocol for the synthesis of quinoline-appended quinazolinones from a reaction of 2-aminoacetophenone, 1,3-cyclohexanedione, and anthranilamide utilizing *p*-TSA as a reagent, and the products thus formed have been evaluated for photophysical properties (Scheme 1, equation 3). It should be noted that both the quinoline and the quinazolinone rings in the products have been formed simultaneously in the one-pot reaction.

RESULTS AND DISCUSSION

At first, 1.0 equiv of each of 2-aminoacetophenone **1a**, 1,3-cyclohexanedione **2a**, and anthranilamide **3a** were treated with 2.0 equiv of *p*-TSA in a sealed tube at 100 °C under a neat condition over 12 h, affording 9-methyl-3,4-dihydro-1′*H*,2*H*-spiro[acridine-1,2′-quinazolin]-4′(3′*H*)-one **4a** in a 17% yield along with an inseparable mixture. Compound **4a** was thoroughly characterized by spectroscopic methods. To prevent the formation of undesired byproducts, the reaction was performed in a periodic addition of the reagents. Thus, initially, a mixture of 1.0 equiv of **1a**, and 1.0 equiv of **2a** was treated with 2.0 equiv of *p*-TSA in a sealed tube and heated at 100 °C for 3 min. Following this, 1.0 equiv of **3a** was added and stirred for 12 h at 100 °C. The reaction yielded **4a** in a 17% yield and a new compound 9-methyl-3,4-dihydroacridin-1(2*H*)-one **5a** in a 74% yield as the major product (Table 1, entry 1).

To improve the yield of **4a**, parameters such as temperature, reagents, the mole ratio of reactants, and solvents were considered. Thus, a reaction with a 1:1 ratio of compounds **1a** and **2a** in the presence of 2 equiv of *p*-TSA at 100 °C for 3 min

https://doi.org/10.1021/acsomega.2c00674
ACS Omega 2022, 7, 20605−20618

Table 1. Optimization of the Synthesis of Compound 4

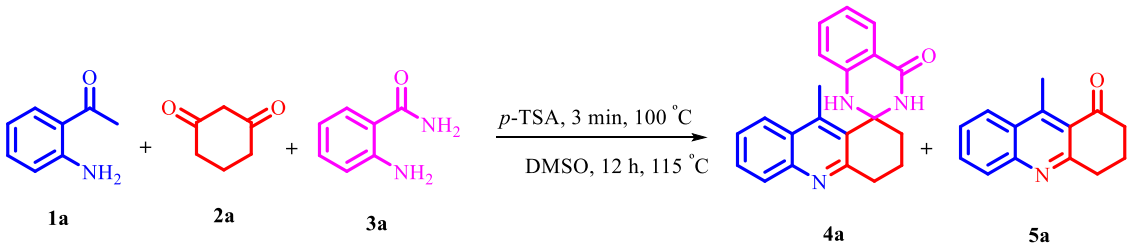

1a 2a 3a 4a 5a

entry	substrate ratio 1a:2a:3a	reagent (equiv)	solvent	temp. °C initial temp., reaction temp.[a]	yield[b] 4a	yield[b] 5a
1	1:1:1	*p*-TSA (2.0)		100, 100	17	74
2	1:1:1	*p*-TSA (2.0)		100, 115	69	23
3	1:1:1	*p*-TSA (2.0)	DMF	115, 115	86	7
4	1:1:1	*p*-TSA (2.0)	1,4-dioxane	100, 115	85	6
5	1:1:1	*p*-TSA (2.0)	toluene	100, 115	83	10
6	1:1:1	*p*-TSA(2.0)	xylene	100, 115	83	10
7[c]	1:1:1	*p*-TSA (2.0)	DMSO	100, 115	87	6
8	1:1:1	$CuSO_4 \cdot 5H_2O$ (2.0)	DMSO	100, 115		32
9	1:1:1	CuI (2.0)	DMSO	100, 115		40
10	1:1:1	$NiCl_2 \cdot 6H_2O$(2.0)	DMSO	100, 115		11
11	1:1:1	AcOH (2.0)	DMSO	100, 115		16
12	1:1:1	$FeCl_3 \cdot 6H_2O$ (2.0)	DMSO	100, 115	30	63
13	1:1:1	Ceralite IR120 (100% W/W)	DMSO	100, 115		
14	1:1:1	MK-10 (100%) W/W	DMSO	100, 115		
15	1:1:1	*p*-TSA (1.0)	DMSO	100, 115	[d]	73
16	1:1:1	*p*-TSA (1.5)	DMSO	100, 115	43	33
17	1:1:1	*p*-TSA (3.0)	DMSO	100, 115	85	10
18	1:1:1.2	*p*-TSA (2.0)	DMSO	100, 115	85	7
19	1.2:1:1	*p*-TSA (2.0)	DMSO	100, 115	84	3
20	1:1.2:1	*p*-TSA (2.0)	DMSO	100, 115	85	6

[a]Reaction was initially carried out at 100 °C for 3 min followed by increasing the temperature to 115 °C. [b]Isolated yield. [c]Optimized condition. [d]Trace.

Scheme 2. Plausible Mechanism for the Formation of Compounds 4 and 5

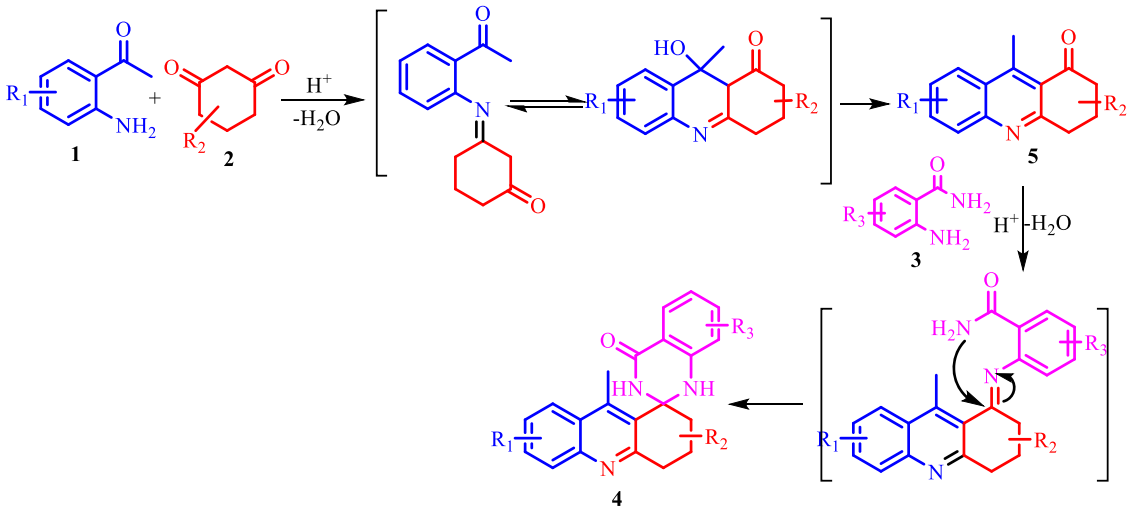

was carried out, followed by the addition of 1 equiv of **3a**, and the temperature was increased to 115 °C. The reaction yielded 69% of **4a** and 23% of **5a**. (Table 1, entry 2). However, we observed that the solvent-free protocol was not suitable for all of the substrates. Hence, various solvents like DMSO, DMF, 1,4-dioxane, toluene, and xylene were introduced to determine the effect of the solvent in facilitating the reaction. The screening of the solvents revealed that the presence of a solvent in the reaction increased the yield of the reaction, but none of the solvents showed a remarkable superiority in the obtained yield. (Table 1, entries 3−7). To choose the best reagents, reagents such as $CuSO_4 \cdot 5H_2O$, CuI, $NiCl_2 \cdot 6H_2O \cdot CH_3COOH$, $FeCl_3.6H_2O$, Ceralite IR120, and MK-10 were screened. None of the above reagents improved the yield (Table 1, entries 8−

https://doi.org/10.1021/acsomega.2c00674
ACS Omega 2022, 7, 20605−20618

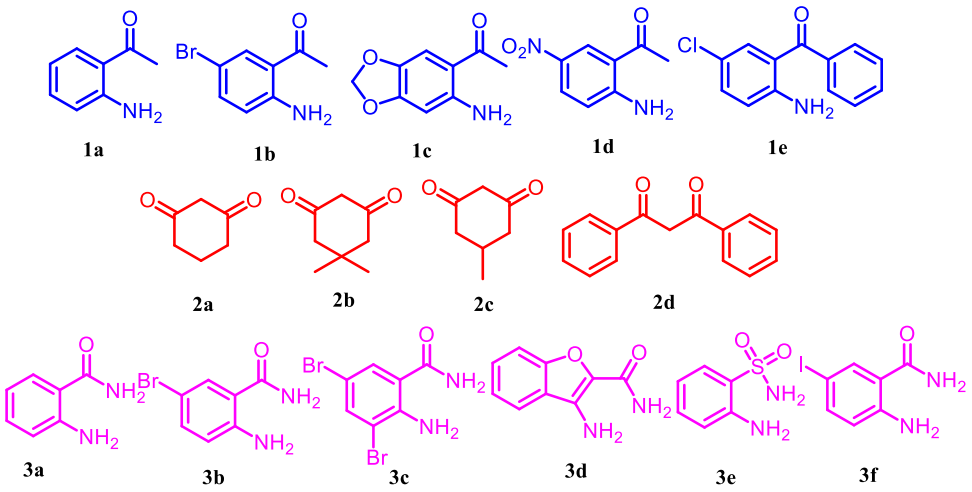

Figure 2. Screening of the starting materials.

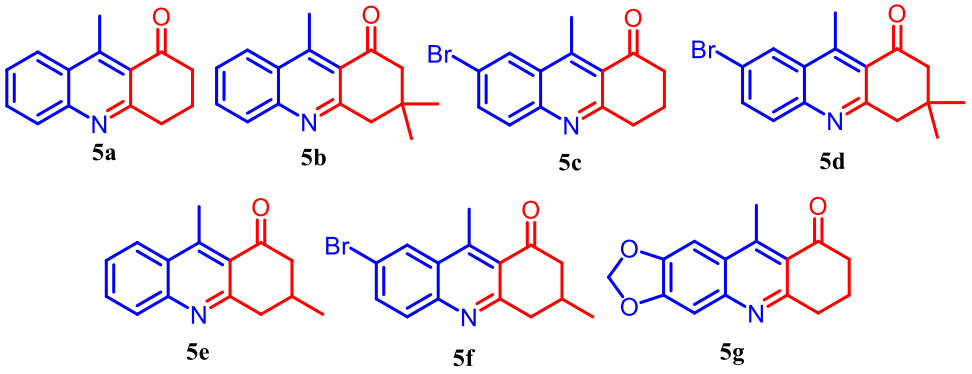

Figure 3. Isolated intermediates.

14). Among the various reagents screened, only $FeCl_3{\cdot}6H_2O$ gave a 30% yield of **4a**. To optimize the amount of *p*-TSA, various equivalents of *p*-TSA were used and the highest yield was obtained with 2 equiv of *p*-TSA (Table 1, entries 15−17). Also, various equivalents of substrates were taken in the presence of 2 equiv of *p*-TSA at 100 °C for 3 min, followed by the addition of **3a,** and the temperature of the reaction system was increased to 115 °C. We observed that no significant improvement in the yield was noticed. However, in all of the cases, a trace of **5a** was observed (Table 1, entries 18−20). Furthermore, to remove the intermittent addition of anthranilamide **3** into the reaction, we performed a reaction by adding all of the reactants (**1**, **2**, and **3**), *p*-TSA, and DMSO together and heating at 100 °C for 3 min, followed by heating at 115 °C over 12 h. We observed no change in the yield percentage of the expected products **4a** and **5a**.

Based on the structure of product **4**, a plausible mechanism is proposed in Scheme 2. Thus, 2-aminoacetophenone **1a** undergoes Friedländer condensation with 1,3-cyclohexanedione **2a** in the presence of *p*-TSA to form an isolable acridinone intermediate **5**. The subsequent reaction of intermediate **5** with anthranilamide **3** forms an imine intermediate, which undergoes intramolecular nucleophilic amide nitrogen attack on the imine, yielding quinoline-appended spiro-quinazolinone **4**. The isolated acridinone intermediate **5** supports the proposed reaction pathway.

The structure of the representative compound **4b** was confirmed by spectroscopic data analysis (see SI), and the relative stereochemistry was assigned based on single-crystal X-ray analysis (Figure 5).[28]

Encouraged by the preliminary results, we investigated the scope of the reaction with several 2-aminoacetophenones, 2-aminoamides, and 1,3-cyclohexanedione (Figures 3−5 and Table 2). Under optimized conditions, (Table 1, entry 7) all of the reactions went smoothly to produce the respective quinoline-appended quinazolinones **4** as the major product and acridinone as the minor product **5**. It was observed that the unsubstituted 2-aminobenzamide **3a** gave a higher yield compared to those with bromine-substituted aminobenzamides **3b** and **3c**. This might be due to the interaction of the bulky Br group with the quinoline methyl in the imine intermediate. The bulky methyl substitutions on the aliphatic ring of the compound did not affect the yield of the reaction. The reaction gave only acridinone **5** as the sole product when the reaction was performed with 3-aminofuran-2-carboxamide and 2-aminobenzene sulfonamide.

The bromine substitutions on the derivatives facilitated further synthetic transformations of the molecules. The effectiveness of this methodology was further scrutinized by a gram-scale synthesis of **4a** under optimized reaction conditions giving a yield of 81%.

To demonstrate the synthetic utility of compounds synthesized, several biphenyl tethered quinoline-appended spiro-quinazolinones were synthesized via the Suzuki coupling reaction, as shown in Scheme 3. Thus, compounds **4c, 4d,** and **4n** were treated with various aryl boronic acids in the presence

https://doi.org/10.1021/acsomega.2c00674
ACS Omega 2022, 7, 20605−20618

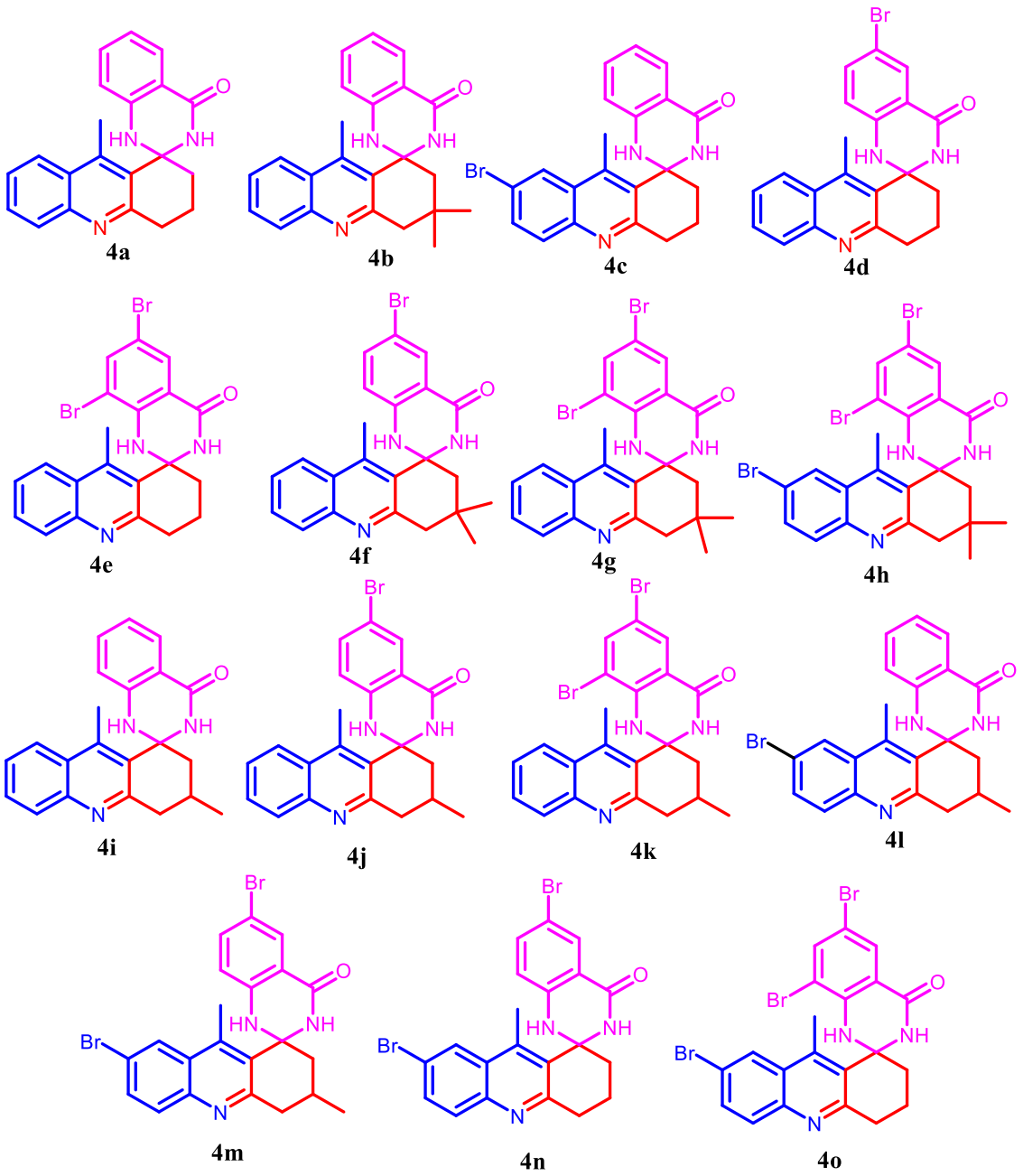

Figure 4. Compounds synthesized.

of $Pd(OAc)_2$ as a catalyst and K_2CO_3 as a base to afford respective arylated products **6a−d** in an 89−95% yield.

Photophysical Studies. The structural uniqueness of quinoline-appended dihydro/spiro-quinazolinones encouraged us to explore their photophysical properties. Thus, compounds **4c** and **4k** were chosen for the investigation. Initially, to establish solvatochromic property, UV−visible spectra of **4c** and **4k** were recorded using solvents such as acetonitrile, methanol, tetrahydrofuran, 1,4-dioxane, and toluene. Two absorption bands were observed in all of the solvents, as shown in Figures 6 and 7. A higher energy band in the range 228 to 287 nm begins with $\pi-\pi^*$ electronic transition [intramolecular charge transfer (ICT)] and other bands with lower energy $n-\pi^*$ electronic transition in the region 345−365 nm were observed. While increasing the solvent polarity from toluene to acetonitrile, a blue shift was observed for both compounds. The wavelength shifted from 287 nm in toluene to 228 nm in acetonitrile to give a shift of 59 nm for compound **4c**. For compound **4k**, a similar shift of 57 nm was observed in the respective solvent. The hypsochromic (blue) shift observed can be associated due to the decrease in the dipole moment in the excited state as compared to the ground state, stabilizing the ground-state energy in polar solvents.[29] Furthermore, the molar extinction coefficient (ε) was calculated using Lambert−Beer's law ($A = \varepsilon cl$). The molar extinction coefficient value of both the derivatives decreased with the decrease in solvent polarity. As the solvent polarity decreased, the value of the molar extinction coefficient of **4c** decreased from 5.1295×10^4 to 0.5664×10^4 $M^{-1}cm^{-1}$ (Table 3). In the case of **4k**, the value of the molar extinction coefficient decreases from 10.3089×10^4 to 1.1268×10^4 $M^{-1}cm^{-1}$ (Table 4).

https://doi.org/10.1021/acsomega.2c00674
ACS Omega 2022, 7, 20605−20618

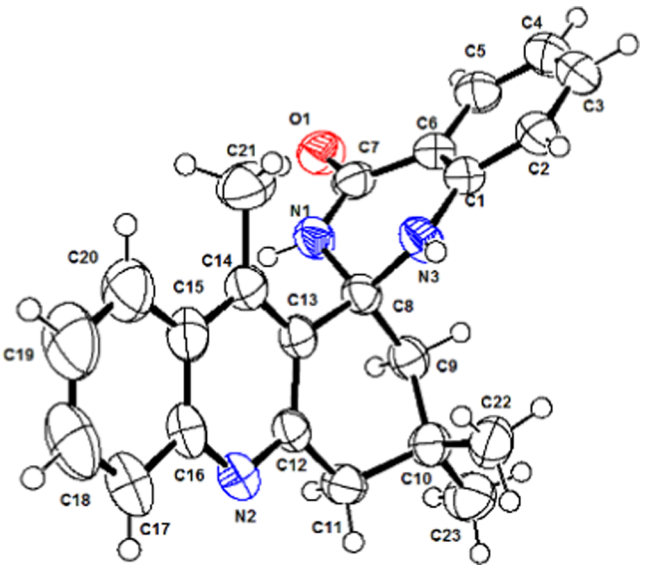

Figure 5. ORTEP diagram of compound **4b**.

Furthermore, the quantum yield and Stoke's shift were calculated for **4c** and **4k** in all of the selected solvents.

Quantum yields of compounds were estimated by comparison with the known quantum yields of anthracene in ethanol (Φ = 0.27) at an excitation wavelength of 246 nm using the equation given in the SI. For compound **4c**, the quantum yield varied from 0.3681 to 0.1063. The highest quantum yield was obtained in acetonitrile. For compound **4k**, the quantum yield varied from 0.8019 to 0.1522 with the highest quantum yield observed in toluene. The Stoke's shift value of compounds **4c** and **4k** in different solvents are given in Tables 3 and 4.

Both the compounds **4c** and **4k** exhibited a large Stoke's shift in the ranges from 20 542 to 12 390 and 21 320 to 10 212 cm^{-1}, which is associated with highly polarizable π-conjugated systems due to ICT. It has also been noted that a large red shift was observed in the excited state when methanol was used as a solvent, as shown in Figures 6 and 7 **1b, 2b**. This might be due to the stronger electron-withdrawing nature of the quinoline ring and the presence of a strong electron-donating amino group in the molecule. Protonation of the compound by the solvent also facilitates the red shift.[30]

The extended π conjugation induced by the aryl system encouraged us to further investigate the photophysical properties of the Suzuki coupled products **6a−d**. Thus, UV−visible and fluorescence spectra of compounds **6a−d** were measured in methanol and the spectra are displayed in Figure 8 a,b. The absorption spectra of compounds **6 a−d** showed two bands in the region of 240−380 nm. The first absorption band is related to higher energy with a lower wavelength $\pi-\pi^*$ transition that appeared in the range of 250−280 nm and another medium energy belonging to the $n-\pi^*$ transition of the compounds appeared as a shoulder in the region of 330−380 nm for compounds **6a−d**. Also, in fluorescence spectra, the medium energy exhibits emission at 367 nm (**6a**), 371 nm (**6b**), 380 nm (**6c**), and 380 nm (**6d**).

Furthermore, Stoke's shift and the molar extinction coefficient for the $\pi-\pi^*$ transition were calculated for **6a−d**. It was observed that the compounds **6a−d** exhibited similar Stoke's shift values. Monoarylated derivatives **6a−b** exhibited

Table 2. Scope of the Reaction

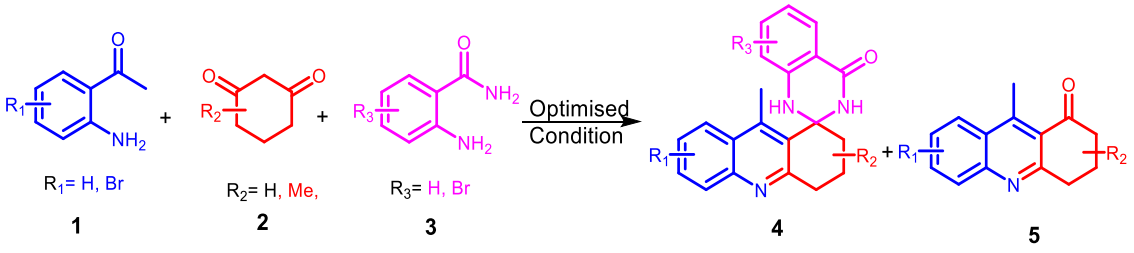

Sl. no	starting materials (1:1:1)			(% Yield)[a,b] 4	5
1	1a	2a	3a	4a (87)	5a (6)
2	1a	2b	3a	4b (85)	5b (7)
3	1b	2a	3a	4c (82)	5c (7)
4	1a	2a	3b	4d (83)	5a (6)
5	1a	2a	3c	4e (82)	5a (8)
6	1a	2b	3b	4f (64)	5b (31)
7	1a	2b	3b	4g (73)	5b (21)
8	1b	2b	3c	4h (6)	5d (81)
9	1a	2c	3a	4i (88)	5e (3)
10	1a	2c	3b	4j (81)	5e (8)
11	1a	2c	3c	4k (79)	5e (10)
12	1b	2c	3a	4l (82)	5f (7)
13	1b	2c	3b	4m (81)	5f (10)
14	1b	2a	3b	4n (86)	5c (5)
15	1b	2a	3c	4o (19)	5c (64)
16	1c	2c	3c		5g (66)

[a]Optimized condition. [b]Isolated yield.

https://doi.org/10.1021/acsomega.2c00674
ACS Omega 2022, 7, 20605−20618

Scheme 3. Synthetic Transformation of Compounds 4c, 4d, and 4n into Biphenyl Derivatives 6a−d

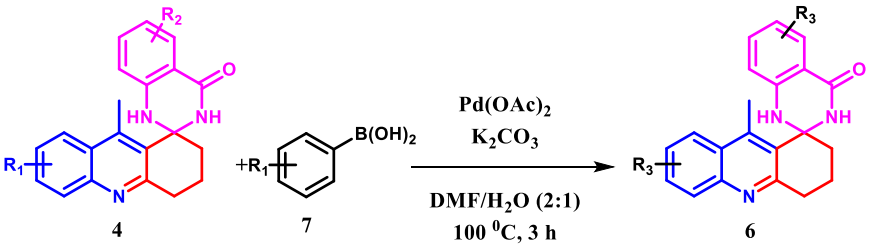

R_1 = H, Br
R_2 = Br, H

R_3= H, Ph, $C_6H_4NO_2$

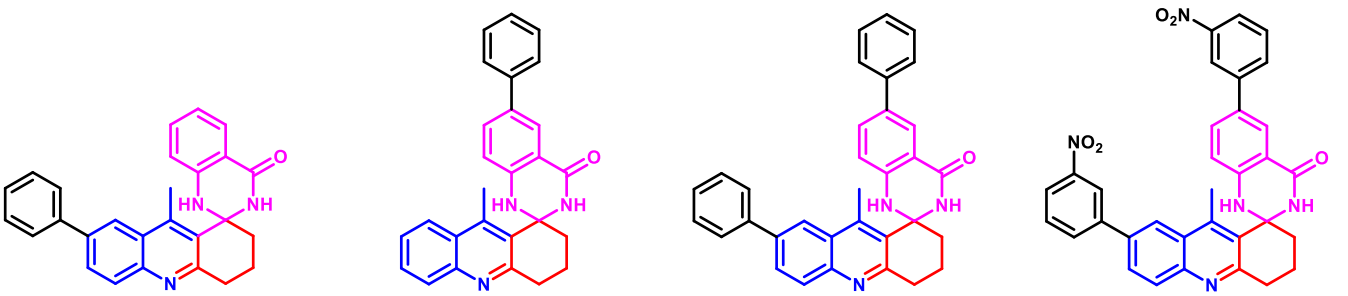

6a (95%) 6b (94%) 6c (92%) 6d (89%)

higher Stoke's shift than the biarylated derivatives **6c−d**. The complete photophysical data along with fluorescence quantum yield (Φ_f) for the synthesized biaryls are summarized in Table 5. It was observed that much increase in the quantum yield was not observed when the phenyl ring was tethered to quinoline-appended quinazolinones.

It was observed that the quantum yield and Stoke's shift values obtained for the quinoline-appended quinazolinones were higher compared to other spiro- and cyclic-quinazolinone heterocyclic derivatives.[31] This class of quinoline-based compounds with a high quantum yield and Stoke's shift values is very useful as labels in biochemical and technical applications.[32]

In conclusion, an efficient one-pot synthesis of quinoline-appended quinazolinone derivatives has been accomplished via Friedländer condensation. A plausible reaction mechanism is provided, and a representative structure of product **4b** was confirmed by XRD. The synthetic utility of the products is demonstrated by the Suzuki coupling reaction. Further, photophysical properties of compounds **4c** and **4k** were evaluated and synthesized biphenyl tethered quinoline-appended quinazolinones were found to be promising blue-emissive fluorescent molecules.

EXPERIMENTAL SECTION

General Remarks. All of the reactions were carried out in oven-dried glassware. Progress of reactions was monitored by thin-layer chromatography (TLC), while purification of crude compounds was done by column chromatography using silica gel (Mesh size 100−200). The NMR spectra were recorded on a Bruker 400 MHz NMR spectrometer (400 MHz for ^{1}H NMR and 100 MHz for ^{13}C NMR) with $CDCl_3$ or $(CD_3)_2SO$ as a solvent and TMS as an internal reference. Integrals are in accordance with assignments; coupling constants were reported in Hertz (Hz). All ^{13}C spectra are proton-decoupled. Multiplicity is indicated as follows: s (singlet), d (doublet), t (triplet), q (quartet), m (multiplet), dd (doublet of doublet), and br s (broad singlet). FTIR spectra were recorded on a Perkin-Elmer RX-I FTIR, and absorbance is reported in cm^{-1}. HRMS analyses were recorded using a Q-Tof Micro mass spectrometer (different mass analyses based on the availability of instruments). Yields refer to quantities obtained after chromatography. Absorption spectra were recorded using a JASCO V-670 spectrophotometer. Steady-state fluorescence spectra were recorded on a Hitachi F-7000 FL Spectro fluorophotometer by excitation at the respective absorption maxima.

Quantum yields of compounds were estimated by comparison with the known quantum yields of anthracene in ethanol (Φ = 0.27) at an excitation wavelength of 246 nm using the following equation:

$$\Phi_f = \Phi_{fR} \cdot I/I_R \cdot OD_R/OD \cdot n^2/n_R^2$$

where Φ is the quantum yield, I is the integrated intensity, OD is the optical density, and n is the refractive index. The subscript R refers to anthracene.

The molar extinction coefficient (ε) was calculated using Lambert−Beer's law

$$A = \varepsilon cl$$

The Stoke's Shift was calculated using the following equation:

$$\Delta\bar{\upsilon} = 10^7/\lambda_{max(absorption)} - 10^7/\lambda_{max(emission)}$$

Experimental Procedures. Compounds **1b**, **3b**, and **3c** were synthesized according to the procedure given in refs 33−35.

*General Procedure for the Synthesis of 2-Amino-5-bromoacetophenone (**1b**).* To a stirred solution of 1-(2-aminophenyl)ethanone (0.5 g, 3.7 mmol) in 5 mL of CH_3CN at 0 °C, *N*-bromosuccinimide (0.66 g, 3.7 mmol) was added dropwise and dissolved in 5 mL of CH_3CN. The mixture was

https://doi.org/10.1021/acsomega.2c00674
ACS Omega 2022, 7, 20605−20618

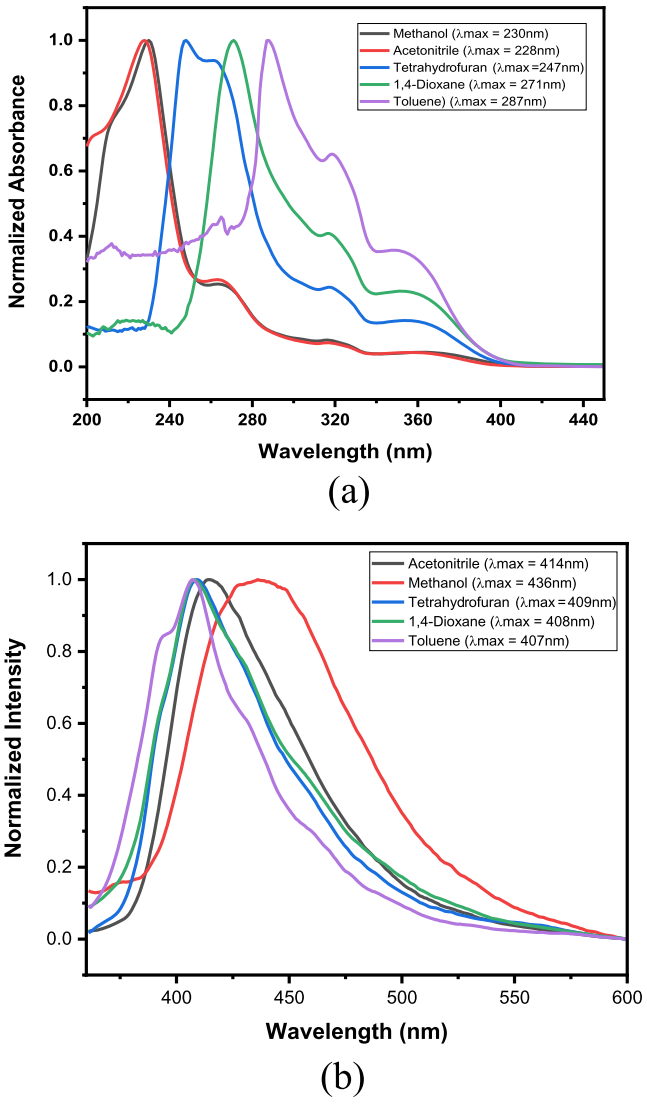

Figure 6. (a) Normalized absorption spectra of compound **4c** recorded at a concentration of 2×10^{-5} M at 298 K and (b) normalized emission spectra of compound **4c** recorded at a concentration of 2×10^{-5} M at 298 K.

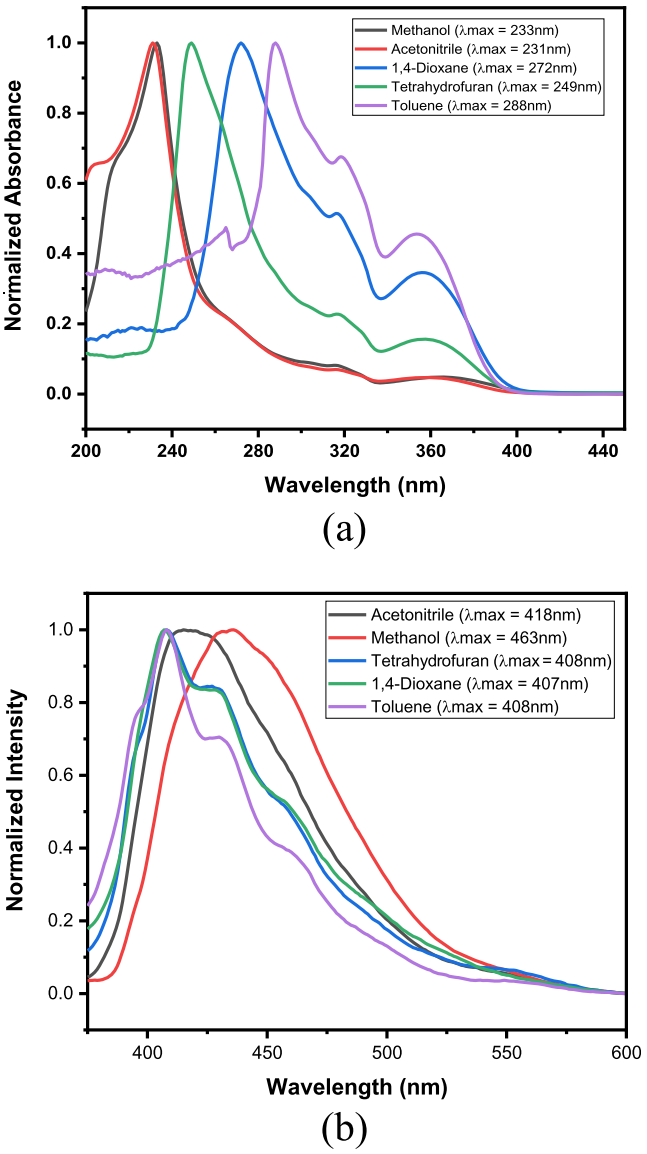

Figure 7. (a) Normalized absorption spectra of compound **4k** recorded at a concentration of 2×10^{-5} M at 298 K and (b) normalized emission spectra of compound **4k** recorded at a concentration of 2×10^{-5} M at 298 K.

allowed to stand at room temperature and continually stirred at room temperature for 3 h. The removal of the solvent under in vacuo and purification through a column of silica gel (petroleum ether/ethyl acetate = 5:1) afforded 1-(2-amino-5-bromophenyl)ethanone.

*General Procedure for the Synthesis of 2-Amino-5-bromobenzamide (**3b**).* In a screw-capped reaction tube, 2-aminobenzamide (0.5 mmol) was dissolved in acetonitrile (2 mL) and *N*-bromosuccinamide (0.6 mmol) dissolved in CH_3CN was added, and the reaction mixture was heated at 60 °C for 10 min. Then, the mixture was diluted with EtOAc and washed with saturated brine. The organic layer separated was dried over anhyd. Na_2SO_4 and concentrated under reduced pressure. The crude compound was purified through a column of silica gel (petroleum ether), affording 1-(2- amino-5-bromophenyl) ethanone.

*General Procedure for the Synthesis of 2-Amino-3,5-dibromobenzamide (**3c**).* In a stirred solution of 2-amino-benzamide (2.0 mmol) in acetonitrile (10.0 mL), *N*-bromosuccinimide (0.85 g, 4.8 mmol, 2.0 equiv) was added, and the reaction mixture was stirred at room temperature for 3 h. The reaction mixture was quenched with crushed ice, resulting in a precipitate. The recrystallization of the residue from MeCN afforded 2-amino-3,5-dibromobenzamide (**3c**).

*General Procedure for the Synthesis of Quinoline-Appended Quinazolinone **4a–o**.* A sealed tube containing 2-aminoacetophenone (1 mmol), 1,3-cyclohexanedione (1.0 mmol), anthranilamide (1.0 mmol), and *p*-toluenesulfoniconic acid (TSA) (2.0 mmol) was heated initially at 100 °C for 5 min. Next, DMSO (300 μL) was added and then the reaction temperature was increased to 115 °C continuously for 12 h. The completion of the reaction was monitored by TLC. The reaction mixture was diluted with water, EtOAc, and washed using a 10% NaOH solution. The combined organic layer was dried over anhyd. Na_2SO_4 and the solvent was evaporated under reduced pressure. The crude mixture was purified by silica gel column chromatography to obtain pure compounds **4a–o**.

https://doi.org/10.1021/acsomega.2c00674
ACS Omega 2022, 7, 20605–20618

Table 3. Photophysical Properties of Compound 4c

entry	solvent	absorption[a] $\lambda_{max,abs}$ (nm)	emission[a] $\lambda_{max,emi}$ (nm)	molar extinction coefficient × 10^4 (ε) π–π^*	Stoke's shift $\Delta\bar{\nu}$ (cm^{-1})[b]	quantum yield (Φ_f)[c]
1	CH_3CN	228, 263	414	5.00985	19 705	0.3681
2	MeOH	230, 264	436	5.12955	20 542	0.3195
3	THF	247, 317	409	1.67091	16 035	0.1063
4	dioxane	271, 317	408	0.97554	12 390	0.2146
5	toluene	287, 319	407	0.56647	10 273	0.2270

[a]Recorded at 298 K. [b]Stoke's shift = $\lambda_{max,abs} - \lambda_{max,emi}$ [cm $^{-1}$]. [c]Determined with anthracene as a standard Φ_f = 0.27 at an excitation wavelength of 246 nm.

Table 4. Photophysical Properties of Compound 4k

entry	solvent	absorption[a] $\lambda_{max,abs}$ (nm)	emission[a] $\lambda_{max,emi}$ (nm)	molar extinction coefficient × 10^4 (ε) π–π^*	Stoke's shift $\Delta\bar{\nu}$ (cm^{-1})[b]	quantum yield (Φ_f)[c]
1	CH_3CN	231	418	7.6462	19 366	0.1522
2	MeOH	233	463	10.3089	21 320	0.1580
3	THF	249, 357	408	3.41119	15 650	0.2754
4	dioxane	272, 356	407	1.54363	12 194	0.7916
5	toluene	288, 353	408	1.12686	10 212	0.8019

[a]Recorded at 298 K. [b]Stoke's shift = $\lambda_{max,abs} - \lambda_{max,emi}$ [cm^{-1}]. [c]Determined with anthracene as a standard Φ_f = 0.27 at an excitation wavelength of 246 nm.

9-Methyl-3,4-dihydro-1′H,2H-spiro[acridine-1,2′-quinazolin]-4′(3′H)-one ***(4a)***. Nature: a brown powder; yield: 87%; R_f (50% EtOAc–hexane): 0.46, M. P: 230–231 °C. FTIR(KBr)-ν_{max}: 3292, 3176, 3049, 1654, 1610, 1512, 1487, 754 cm^{-1}; ^{1}H NMR (400 MHz, DMSO-d_6): δ 8.31 (s, 1H), 8.16 (d, J = 8.5 Hz, 1H), 7.88 (d, J = 8.4 Hz, 1H), 7.71 (t, J = 7.6 Hz, 1H), 7.65 (d, J = 7.9 Hz, 1H), 7.54 (t, J = 7.6 Hz, 1H), 7.29 (s, 1H), 7.24 (t, J = 7.6 Hz, 1H), 6.65 (dd, J = 7.7, 4.3 Hz, 2H), 3.10–2.95 (m, 2H), 2.91 (s, 3H), 2.35–2.06 (m, 3H), 2.00–1.79 (m, 2H). ^{13}C NMR (101 MHz, DMSO-d_6): δ 162.2, 158.1, 146.6, 146.2, 146.0, 133.6, 130.3, 129.6, 128.4, 127.7, 127.3, 125.7, 124.2, 116.4, 114.2, 113.2, 70.2, 34.7, 31.5, 29.4, 16.3. HRMS-ESI: calcd for $C_{21}H_{19}N_3O$ $[M + H]^+$ m/z: 330.1606; found: 330.1614.

Isolated Intermediate: **5a** (6%).

3,3,9-Trimethyl-3,4-dihydro-1′H,2H-spiro[acridine-1,2′-quinazolin]-4′(3′H)-one ***(4b)***. Nature: a brown powder; yield: 85%; R_f (50% EtOAc–hexane): 0.48, M. P: 240–241 °C. FTIR(KBr)ν_{max}: 3259, 3062, 2922, 1633, 1606, 1510, 1357, 745 cm^{-1}; ^{1}H NMR (400 MHz, DMSO-d_6):δ 8.26–8.10 (m, 2H), 7.91 (d, J = 8.1 Hz, 1H), 7.75–7.55 (m, 3H), 7.25 (t, J = 7.1 Hz, 1H), 6.93 (s, 1H), 6.67 (t, J = 7.2 Hz, 2H), 2.97 (s, 3H), 2.89 (s, 2H), 2.35–2.22 (m, 2H), 1.03 (s, 6H). ^{13}C NMR (101 MHz, DMSO-d_6): δ 163.4, 157.5, 148.5, 147.4, 145.1, 134.6, 130.5, 129.2, 128.7, 128.5, 127.4, 126.4, 124.3, 119.1, 114.5, 114.1, 77.4, 77.3, 77.1, 71.9, 52.5, 49.3, 30.0, 29.2, 27.6, 17.0. HRMS-ESI: calcd for $C_{23}H_{23}N_3O$ $[M + H]^+$ m/z: 358.1919; found: 358.1938.

Isolated Intermediate: **5b** (7%).

7-Bromo-9-methyl-3,4-dihydro-1′H,2H-spiro[acridine-1,2′-quinazolin]-4′(3′H)-one ***(4c)***. Nature: a brown powder; yield: 82%; R_f (50% EtOAc–hexane): 0.50, M. P: 265–266°C. FTIR(KBr)ν_{max}: 3284, 3064, 2924, 2852, 1658, 1606, 1481, 759 cm^{-1}; ^{1}H NMR (400 MHz, DMSO-d_6) δ: 8.44 (s, 1H), 8.10 (d, J = 8.4 Hz, 1H), 7.82 (d, J = 8.3 Hz, 1H), 7.66 (dd, J = 7.8, 4.8 Hz, 2H), 7.49 (t, J = 7.2 Hz, 2H), 7.33 (dd, J = 8.7, 2.4 Hz, 1H), 6.57 (d, J = 8.7 Hz, 1H), 2.96–2.89 (m, 2H), 2.81 (s, 3H), 2.29–1.99 (m, 2H), 1.83 (s, 2H). ^{13}C NMR (101 MHz, DMSO-d_6) δ: 161.0, 158.1, 146.7, 146.3, 145.0, 136.1, 129.8, 129.4, 128.4, 127.7, 125.9, 124.3, 116.6, 114.8, 107.3, 70.3, 62.8, 34.7, 21.1, 17.1, 16.3. HRMS-ESI: calcd for $C_{21}H_{18}BrN_3O$ $[M + H]^+$ m/z: 408.0711; found: 408.0713.

Isolated Intermediate: **5c** (7%).

6′-Bromo-9-methyl-3,4-dihydro-1′H,2H-spiro[acridine-1,2′-quinazolin]-4′(3′H)-one ***(4d)***. Nature: a brown powder; yield: 83%; R_f (50% EtOAc–hexane): 0.51, M. P: 270–271°C. FTIR(KBr)ν_{max}: 3284, 2922, 2850, 1656, 1604, 1481, 759 cm^{-1}; ^{1}H NMR (400 MHz, DMSO-d_6) δ: 8.48 (s, 1H), 8.14 (d, J = 8.4 Hz, 1H), 7.86 (d, J = 8.2 Hz, 1H), 7.73–7.66 (m, 2H), 7.57–7.49 (m, 2H), 7.36 (dd, J = 8.6, 2.4 Hz, 1H), 6.61 (d, J = 8.7 Hz, 1H), 2.98 (dd, J = 14.0, 7.5 Hz, 2H), 2.85 (s, 3H), 2.33–2.04 (m, 2H), 1.87 (t, J = 6.7 Hz, 2H). ^{13}C NMR (101 MHz, DMSO-d_6) δ: 161.0, 158.1, 146.7, 146.3, 145.0, 136.1, 129.9, 129.8, 129.4, 128.4, 127.7, 125.9, 124.3, 116.6, 114.8, 107.3, 70.3, 62.8, 34.7, 17.1, 16.3. HRMS-ESI: calcd for $C_{21}H_{18}BrN_3O$ $[M + H]^+$ m/z: 408.0711; found: 408.0741.

Isolated Intermediate: **5a** (6%).

6′,8′-Dibromo-9-methyl-3,4-dihydro-1′H,2H-spiro[acridine-1,2′-quinazolin]-4′(3′H)-one ***(4e)***. Nature: a white powder; yield: 82%; R_f (50% EtOAc–hexane): 0.47, M. P: 265–266 °C. FTIR(KBr)ν_{max}: 3338, 3163, 3037, 2939, 1656, 1600, 1489, 752 cm^{-1}; ^{1}H NMR (400 MHz, DMSO-d_6) δ: 8.83 (s, 1H), 8.18 (d, J = 8.2 Hz, 1H), 7.91 (d, J = 8.2 Hz, 1H), 7.82 (m, 2H), 7.79–7.70 (m, 1H), 7.61–7.53 (m, 1H), 6.98 (s, 1H), 3.04 (t, J = 6.2 Hz, 2H), 2.85 (s, 3H), 2.51–2.23 (m, 2H), 2.10–1.92 (m, 2H). ^{13}C NMR (101 MHz, DMSO-d_6) δ: 159.9, 158.4, 146.3, 145.9, 142.5, 138.2, 129.6, 129.2, 128.4, 127.7, 125.6, 124.1, 116.2, 108.3, 107.3, 70.6, 34.6, 16.9, 16.2. HRMS-ESI: calcd for $C_{21}H_{17}Br_2N_3O$ $[M + H]^+$ m/z: 485.9816; found: 485.9814.

Isolated Intermediate: **5a** (8%).

6′-Bromo-3,3,9-trimethyl-3,4-dihydro-1′H,2H-spiro[acridine-1,2′-quinazolin]-4′(3′H)-one ***(4f)***. Nature: white powder; yield: 64%; R_f (50% EtOAc–hexane): 0.46, M. P: 257–258 °C. FTIR(KBr)ν_{max}: 3186, 3066, 2962, 1656, 1608, 1500, 754 cm^{-1}; ^{1}H NMR (400 MHz, DMSO-d_6) δ: 8.35 (s, 1H), 8.20 (d, J = 8.5 Hz, 1H), 7.91 (d, J = 8.4 Hz, 1H), 7.78–7.70 (m, 2H), 7.57 (t, J = 7.6 Hz, 1H), 7.40 (d, J = 8.7 Hz, 1H), 7.21 (s, 1H), 6.63 (d, J = 8.7 Hz, 1H), 2.93 (s, 3H), 2.88 (s, 2H), 2.27 (m, 1H), 1.90 (s, 1H), 1.02 (d, J = 1.8 Hz, 6H).

https://doi.org/10.1021/acsomega.2c00674
ACS Omega 2022, 7, 20605–20618

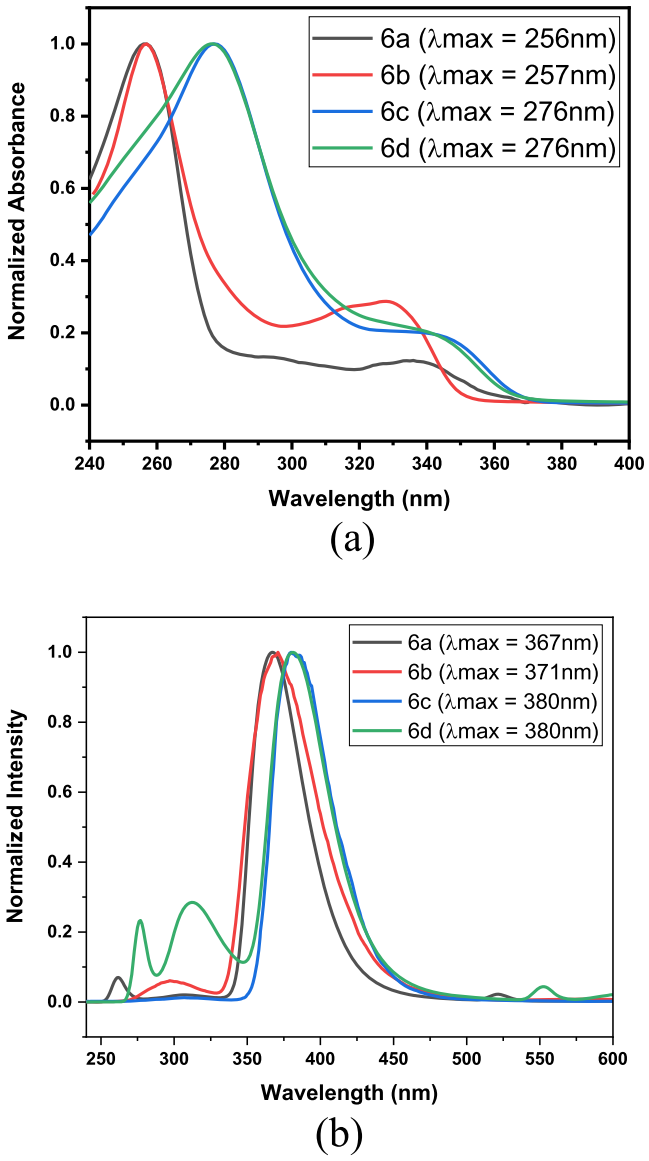

Figure 8. (a) Normalized absorption spectra of compounds **6a−d** recorded at a concentration of 2 × 10^{-5} M at 298 K and (b) normalized emission spectra of compounds **6a−d** recorded at a concentration of 2 × 10^{-5} M at 298 K.

^{13}C NMR (101 MHz, DMSO-d_6) δ: 171.9, 161.1, 157.5, 146.9, 146.6, 144.9, 136.0, 129.7, 129.3, 128.6, 127.9, 127.8, 125.9, 124.3, 116.7, 115.1, 107.3, 70.1, 52.1, 48.7, 29.5, 27.4, 21.0, 16.3. HRMS-ESI: calcd for $C_{23}H_{22}BrN_3O$ $[M + H]^+$ m/z: 436.1024; found: 436.1037.

Isolated Intermediate: **5b** (31%).

6′,8′-Dibromo-3,3,9-trimethyl-3,4-dihydro-1′H,2H-spiro-[acridine-1,2′-quinazolin]-4′(3′H)-one ***(4g)***. Nature: a yellow powder; yield: 73%; R_f (50% EtOAc−hexane): 0.50, M. P: 239−240 °C. FTIR(KBr)ν_{max}: 3423, 3167, 3066, 2920, 1662, 1598, 1487, 750 cm^{-1}; ^{1}H NMR (400 MHz, $CDCl_3$) δ: 8.29 (d, J = 1.7 Hz, 1H), 8.01−7.93 (m, 2H), 7.68−7.61 (m, 2H), 7.44 (t, J = 7.6 Hz, 2H), 7.34 (t, J = 7.4 Hz, 1H), 3.12 (s, 2H), 3.04 (s, 3H), 2.61 (s, 2H), 1.07 (d, J = 4.9 Hz, 6H). ^{13}C NMR (101 MHz, $CDCl_3$) δ: 161.4, 157.3, 141.4, 139.1, 130.8, 129.1, 128.4, 126.6, 124.3, 116.3, 110.4, 109.4, 72.0, 52.8, 49.0, 30.0, 27.2, 17.0. HRMS-ESI: calcd for $C_{23}H_{21}Br_2N_3O$ $[M + H]^+$ m/z: 514.0129; found: 514.0124.

Isolated Intermediate: **5b** (21%).

6′,7,8′-Tribromo-3,3,9-trimethyl-3,4-dihydro-1′H,2H-spiro[acridine-1,2′-quinazolin]-4′(3′H)-one ***(4h)***. Nature: a brown powder; yield: 6%; R_f (50% EtOAc−hexane): 0.46, M. P: 212−213 °C. FTIR(KBr)ν_{max}: 3192, 3072, 2922, 1662, 1598, 1463, 796 cm^{-1}; ^{1}H NMR (400 MHz, $CDCl_3$) δ: 8.25 (dd, J = 13.1, 1.7 Hz, 1H), 8.10−8.02 (m, 1H), 7.94−7.85 (m, 1H), 7.59 (m, 1H), 7.52−7.44 (m, 1H), 7.40 (dt, J = 9.7, 5.6 Hz, 1H), 7.37−7.25 (m, 1H), 3.16 (t, J = 9.3 Hz, 2H), 3.03 (t, J = 2.6 Hz, 3H), 2.58 (d, J = 5.5 Hz, 2H), 1.05 (d, J = 4.8 Hz, 6H). ^{13}C NMR (101 MHz, $CDCl_3$) δ: 161.6, 157.7, 141.3, 139.3, 138.7, 134.5, 130.7, 129.7, 126.8, 116.2, 110.6, 109.5, 71.8, 52.7, 30.0, 29.8, 27.3, 17.2, 17.1. HRMS-ESI: calcd for $C_{23}H_{20}Br_3N_3O$ $[M + H]^+$ m/z: 591.9235; found: 591.9231.

Isolated intermediate: **5d** (81%).

3,9-Dimethyl-3,4-dihydro-1′H,2H-spiro[acridine-1,2′-quinazolin]-4′(3′H)-one ***(4i)***. Nature: a pale yellow powder; yield: 88%; R_f (50% EtOAc−hexane): 0.48, M. P: 274−275 °C. FTIR(KBr)ν_{max}: 3290, 3174, 2924, 1658, 1612, 1485, 756 cm^{-1}; ^{1}H NMR (400 MHz, DMSO-d_6) δ: 8.52 (s, 1H (D_2O exchangeable)), 8.18 (d, J = 4 Hz, 1H) 8.17 (s, 1H (D_2O exchangeable)), 7.89 (d, J = 12 Hz, 1H), 7.73 (t, J = 7.6Hz, 1H), 7.68−7.63 (m, 1H), 7.56 (t, J = 7.6Hz, 1H), 7.39 (s, 1H (D_2O exchangeable)), 7.25 (t, J = 7.6 Hz, 1H), 7.05 (s, 1H (D_2O exchangeable)) 6.69−6.61 (m, 2H), 3.13−3.07 (m, 1H), 2.64−2.58 (m, 2H), 2.27−2.23 (m, 1H), 1.65 (t, J = 12.8, 1H), 1.05−1.01 (m, 3H). ^{13}C NMR (101 MHz, DMSO-d_6) δ: 162.2, 157.9, 146.5, 146.4, 146.3, 145.7, 133.6, 133.5, 129.6, 129.6, 128.5, 127.7, 127.3, 127.3, 125.7, 124.2, 124.1, 116.51, 116.2, 114.1, 114.0, 113.2, 70.7, 70.6, 48.7, 43.5, 43.3, 40.1, 38.8, 23.8, 22.9, 21.1, 21.1, 16.1. HRMS-ESI: calcd for $C_{22}H_{21}N_3O$ $[M + H]^+$ m/z: 344.1763; found: 344.1779.

Isolated Intermediate: **5e** (3%)

6′-Bromo-3,9-dimethyl-3,4-dihydro-1′H,2H-spiro-[acridine-1,2′-quinazolin]-4′(3′H)-one ***(4j)***. Nature: a white powder; yield: 81%; R_f (50% EtOAc−hexane): 0.50, M. P: 279−280 °C. FTIR(KBr)ν_{max}: 3188, 3062, 2926, 1660, 1610, 1481, 756 cm^{-1}; ^{1}H NMR (400 MHz, DMSO-d_6): δ 8.71 (s, 1H), 8.38 (s, 1H), 8.19 (d, J = 8.4 Hz, 1H), 7.91 (d, J = 8.3

Table 5. Photophysical Properties of Biaryl Derivatives 6a−d

entry	product	absorption[a] $\lambda_{max,abs}$ (nm)	emission[a] $\lambda_{max,emi}$ (nm)	molar extinction coefficient × 10^4 (ε) $\pi-\pi^*$	Stoke's shift $\Delta\bar{\nu}$ (cm^{-1})[b]	quantum yield (Φ_f)[c]
1	**6a**	256, 334	367	2.0435	11 814	0.1676
2	**6b**	257, 328	371	5.0952	11 956	0.1212
3	**6c**	276	380	4.5657	9916	0.1755
4	**6d**	276	380	6.0996	9916	0.0359

[a]Recorded in MeOH at 298 K. [b]Stoke's shift = $\lambda_{max,abs} - \lambda_{max,emi}$ [cm^{-1}]. [c]Determined with anthracene as a standard Φ_f = 0.27 at an excitation wavelength of 246 nm.

https://doi.org/10.1021/acsomega.2c00674
ACS Omega 2022, 7, 20605−20618

Hz, 1H), 7.76−7.70 (m, 2H), 7,65 (s, 1H), 7.57 (t, J = 7.6Hz, 1H), 7.40 (d, J = 8.8 Hz, 1H), 7.33 (s, 1H), 6.66−6.60 (m, 1H), 3.14−3.09 (m, 1H), 2.89 (d, J = 6 Hz, 3H), 2.67−2.53 (m, 2H), 2.25−2.20 (m, 1H), 1.70−1.63 (m, 1H), 1.04 (t, J = 7.2Hz, 3H). ^{13}C NMR (101 MHz, DMSO-d_6): δ 160.9, 157.7, 146.3, 144.7, 136.0, 129.7, 129.3, 129.2, 128.5, 127.7, 125.8, 124.2, 116.6, 114.9, 107.4, 70.7, 47.9, 43.2, 23.8, 21.0, 16.1. HRMS-ESI: calcd for $C_{22}H_{20}BrN_3O$ $[M + H]^+$ m/z: 422.0868; found: 422.0900.

Isolated Intermediate: **5e** (8%).

6′,8′-Dibromo-3,9-dimethyl-3,4-dihydro-1′H,2H-spiro-[acridine-1,2′-quinazolin]-4′(3′H)-one ***(4k)***. Nature: a brown powder; yield: 79%; R_f (50% EtOAc−hexane): 0.45, M. P: 268−269 °C. FTIR(KBr)ν_{max}: 3192, 3062, 2922, 1664, 1598, 1483, 756 cm^{-1}; ^{1}H NMR (400 MHz, DMSO-d_6): δ 8.93 (s, 1H), 8.65 (s, 1H), 8.17 (d, J = 8.8 Hz, 1H), 7.90 (d, J = 8.4 Hz, 1H), 7.82−7.77 (m, 2H), 7.73 (t, J = 7.2 Hz, 1H), 7.56 (t, J = 7.6Hz, 1H), 7.02 (s, 1H), 6.89 (s, 1H), 3.13−3.05 (m, 1H), 2.83 (d, J = 6.8 Hz, 3H), 2.69−2.58 (m, 2H), 2.28−2.24 (m, 1H), 1.92−1.64 (m, 1H), 1.05−1.01 (m, 3H). ^{13}C NMR (101 MHz, DMSO-d_6): δ 159.6, 158.3, 158.2, 146.4, 142.8, 142.1, 138.3, 129.6, 129.5, 129.2, 128.5, 128.4, 125.6, 124.2, 124.1, 116.8, 115.5, 108.5, 108.1, 107.7, 71.2, 70.9, 48.5, 47.9, 43.3, 43.2, 23.6, 22.9, 21.1, 21.0, 16.3, 15.9. HRMS-ESI: calcd for $C_{22}H_{19}Br_2N_3O$ $[M + H]^+$ m/z: 499.9973; found: 499.9970.

Isolated Intermediate: **5e** (10%).

7-Bromo-3,9-dimethyl-3,4-dihydro-1′H,2H-spiro[acridine-1,2′-quinazolin]-4′(3′H)-one ***(4l)***. Nature: a white powder; yield: 82%; R_f (50% EtOAc−hexane): 0.53, M. P: 276−278 °C. FTIR(KBr)ν_{max}: 3194, 3066, 2926, 1660, 1610, 1498, 756 cm^{-1}; ^{1}H NMR (400 MHz, DMSO-d_6): δ 8.71 (s, 1H), 8.38 (s, 1H), 8.19 (d, J = 8.4 Hz, 1H), 7.91 (d, J = 8.2 Hz, 1H), 7.72 (d, J = 11.2Hz, 2H), 7.65 (s, 1H) 7.58 (t, J = 8.0Hz, 1H), 7.40 (d, J = 8.0Hz, 1H), 7.33 (s, 1H), 6.66−6.60 (m, 1H), 3.12 (d, J = 15.6 Hz, 1H), 2.89 (s, 3H), 2.68−2.50 (m, 2H), 2.23 (s, 1H), 1.70−1.64 (m, 1H), 1.03 (d, J = 6.2 Hz, 3H). ^{13}C NMR (101 MHz, DMSO-d_6): δ 160.9, 157.7, 146.3, 144.7, 136.0, 129.7, 129.3, 129.2, 124.2, 116.6, 114.9, 107.4, 70.7, 23.8, 21.0, 16.1. HRMS-ESI: calcd for $C_{22}H_{20}BrN_3O$ $[M + H]^+$ m/z: 422.0868; found: 422.0886.

Isolated Intermediate: **5f** (7%).

6′,7-Dibromo-3,9-dimethyl-3,4-dihydro-1′H,2H-spiro-[acridine- 1,2′-quinazolin]-4′(3′H)-one ***(4m)***. Nature: a yellow powder; yield: 81%; R_f (50% EtOAc−hexane): 0.51, M. P: 280−281 °C. FTIR(KBr)ν_{max}: 3304, 3062, 2924, 1674, 1604, 1479, 831 cm^{-1}; ^{1}H NMR (400 MHz, DMSO-d_6): δ 8.72 (s, 1H), 8.38 (s, 1H), 7.85 (s, 2H), 7.74−7.70 (m, 1H), 7.76 (s, 1H), 7.37 (t, J = 8.0 Hz, 1H), 6.65−6.59 (m, 1H), 5.75 (s, 1H), 3.12−3.06 (m, 1H), 2.86 (d, J = 8.0 Hz, 3H), 2.66−2.56 (m, 2H), 2.26−2.20 (m, 1H), 1.69−1.62 (m, 1H), 1.03 (t, J = 7.0 Hz, 3H). ^{13}C NMR (101 MHz, DMSO-d_6): δ 160.6, 158.8, 158.6, 146.1, 145.4, 145.0, 144.6, 136.0, 132.8, 130.7, 130.3, 130.2, 129.3, 129.3, 129.1, 126.4, 126.4, 119.1, 119.0, 116.6, 116.5, 114.8, 107.4, 107.1, 70.7, 70.6, 54.8, 43.1, 23.7, 22.7, 20.9, 20.9, 16.2, 16.1. HRMS-ESI: calcd for $C_{22}H_{19}Br_2N_3O$ $[M + H]^+$ m/z: 499.9973; found: 499.9973.

Isolated Intermediate: **5f** (10%).

6′,7-Dibromo-9-methyl-3,4-dihydro-1′H,2H-spiro-[acridine-1,2′-quinazolin]-4′(3′H)-one ***(4n)***. Nature: a brown powder; yield: 86%; R_f (50% EtOAc−hexane): 0.49, M. P: 260−261 °C. FTIR(KBr)ν_{max}: 3305, 3062, 2933, 1666, 1604, 1492, 1315, 835 cm^{-1}; ^{1}H NMR (400 MHz, DMSO-d_6): δ 8.52 (s, 1H), 8.38 (s, 1H), 8.31 (s, 1H), 7.85 (s, 1H), 7.72 (d, J = 2.4 Hz, 1H), 7.58 (s, 1H), 7.42−7.39 (m, 1H), 6.64 (d, J = 8.4Hz, 1H), 3.07−3.00 (m, 2H), 2.86 (s, 3H), 2.34−2.29 (m, 1H), 2.16−2.14 (m, 1H), 1.94−1.88 (m, 1H) ^{13}C NMR (101 MHz, DMSO-d_6): δ 160.8, 158.9, 146.1, 144.9, 144.9, 136.0, 132.8, 130.8, 130.7, 129.3, 129.1, 126.4, 119.0, 116.5, 114.7, 107.3, 79.1, 70.2, 34.6, 16.9, 16.2. HRMS-ESI: calcd for $C_{21}H_{17}Br_2N_3O$ $[M + H]^+$ m/z: 485.9816; found: 488.9835.

Isolated Intermediate: **5c** (5%).

6′,7,8′-Tribromo-9-methyl-3,4-dihydro-1′H,2H-spiro [acridine-1,2′-quinazolin]-4′(3′H)-one ***(4o)***. Nature: a brown powder; yield: 19%; R_f (50% EtOAc−hexane): 0.50, M. P: 207−208 °C. FTIR(KBr)ν_{max}: 3194, 3059, 2924, 1666, 1598, 1481,825 cm^{-1}; ^{1}H NMR (400 MHz, DMSO-d_6): δ 8.83 (s, 1H), 8.37 (s, 1H), 8.32 (s, 1H), 7.85−7.79 (m, 4H), 7.01 (s, 1H), 3.01 (t, J = 6.0Hz, 2H), 2.81 (s, 3H), 2.32−2.19 (m, 1H), 1.19 (s, 2H). ^{13}C NMR (101 MHz, DMSO-d_6): δ 162.2, 158.1, 146.6, 146.2, 146.0, 133.6, 130.3, 129.6, 128.4, 127.7, 127.3, 125.7, 124.2, 116.4, 114.1, 113.2, 70.2, 34.7, 31.5, 17.1, 16.3. HRMS-ESI: calcd for $C_{21}H_{16}Br_3N_3O$ $[M + H]^+$ m/z: 563.8921; found: 563.8931.

Isolated intermediate: **5c** (64%).

Gram-Scale Synthesis of ***4a***. A 100 mL sealed tube containing 1 g (0.900 mL) of 2-aminoacetophenone, 0.830 g of 1,3-cyclohexanedione, 1.007 g of 2-aminobenzamide, and 2.548 g of p-TSA was heated initially at 100 °C for 5 min. Next, DMSO (3 mL) was added and then the reaction temperature was increased to 115 °C continuously for 12 h. The completion of the reaction was monitored by TLC. The reaction mixture was diluted with water, EtOAc, and washed using a 10% NaOH solution. The combined organic layer was dried over anhyd. Na_2SO_4 and the solvent was evaporated under reduced pressure. The crude mixture was purified by silica gel column chromatography to obtain pure compound **4a** (1.973 g) in an 81% yield and compound **5a** (0.172 g) in an 11% yield.

General Procedure for the Synthesis of Compounds ***6a and 6b***. A mixture of compound **4d** or **4c** (0.191 mmol), aryl boronic acids (0.286 mmol), $Pd(OAc)_2$ (10 mol %), and K_2CO_3 (0.286 mmol) in 2 mL of DMF−H_2O (3:1) was stirred at 100 °C for 3 h in a sealed tube. After the completion of the reaction (TLC), the residue was diluted with EtOAc and washed with HCl (0.25 M, 20 mL), followed by saturated brine. The combined organic layer was dried over anhyd. Na_2SO_4 and purified through silica gel column chromatography by gradient elution using EtOAc/hexane to afford compounds **6a−6b** in good yields.

9-Methyl-7-phenyl-3,4-dihydro-1′H,2H-spiro[acridine-1,2′-quinazolin]-4′(3′H)-one ***(6a)***. Nature: a red powder; yield: 95%; R_f (30% EtOAc−hexane): 0.50, M.P: 240−242°C. FTIR(KBr)ν_{max}: 3408, 3192, 2922, 1658, 1608, 1483, 756 cm^{-1}; ^{1}H NMR (400 MHz, $CDCl_3$): δ 8.08 (d, J = 6.8 Hz, 1H), 7.99−7.89 (m, 1H), 7.86 (d, J = 8.8 Hz, 2H), 7.58 (d, J = 6.9 Hz, 2H), 7.41 (t, J = 7.3 Hz, 2H), 7.32 (m, 1H), 7.27 (t, J = 7.6 Hz, 1H), 6.77 (d, J = 3.2 Hz, 1H), 6.61 (d, J = 8.0 Hz, 1H), 6.13 (s, 1H), 3.11 (s, 2H), 3.00−2.87 (m, 3H), 2.36 (m, 2H), 1.88 (s, 2H). ^{13}C NMR (101 MHz, $CDCl_3$): δ 163.4, 157.9, 145.0, 140.5, 134.6, 129.3, 129.1, 128.7, 128.4, 127.9, 127.6, 122.0, 119.0, 114.7, 114.1, 39.7, 29.8, 18.2, 17.2 HRMS-ESI: calcd for $C_{27}H_{23}N_3O$ $[M + H]^+$ m/z: 406.1919; found 406.1923.

9-Methyl-6′-phenyl-3,4-dihydro-1′H,2H-spiro[acridine-1,2′-quinazolin]-4′(3′H)-one ***(6b)***. Nature: a brown powder; yield: 94%; R_f (30% EtOAc−hexane): 0.49, M.P: 259−260 °C.

https://doi.org/10.1021/acsomega.2c00674
ACS Omega 2022, 7, 20605−20618

FTIR(KBr)ν_{max}: 3246, 3051, 2935, 1645, 1614, 1481, 754 cm^{-1}; ^1H NMR (400 MHz, $CDCl_3$): δ 8.35 (d, J = 8.5 Hz, 2H), 8.07 (d, J = 8.3 Hz, 1H), 7.97 (d, J = 8.7 Hz, 1H), 7.84 (d, J = 7.3 Hz, 2H), 7.65 (m, 1H), 7.51 (t, J = 7.6 Hz, 2H), 7.40 (t, J = 7.3 Hz, 1H), 7.31 (s, 1H), 7.28−7.20 (m, 1H), 6.65 (m, 1H), 3.03 (m, 2H), 3.00 (s, 3H), 2.23 (m, 2H), 2.05−1.81 (m, 2H). ^{13}C NMR (101 MHz, $CDCl_3$): δ 161.4, 157.3, 141.4, 139.1, 130.8, 130.7, 129.1, 128.4, 126.6, 124.3, 116.3, 110.4, 109.4, 72.0, 52.8, 49.0, 27.1, 17.0 HRMS-ESI: calcd for $C_{27}H_{23}N_3O$ $[M + H]^+$ m/z: 406.1919; found 406.1927.

General Procedure for the Synthesis of Compounds ***6c*** *and* ***6d***. A mixture of compound **4n** (0.191 mmol), aryl boronic acids (0.573 mmol), $Pd(OAc)_2$ (20 mol %), and K_2CO_3 (0.573 mmol) in 2 mL of DMF−H_2O (3:1) was stirred at 100 °C for 3 h in a sealed tube. After the completion of the reaction (TLC), the residue was diluted with EtOAc and washed with HCl (0.25 M, 20 mL), followed by saturated brine. The combined organic layer was dried over anhydrous Na_2SO_4 and purified through silica gel column chromatography by gradient elution using EtOAc/hexane to afford compounds **6c**−**6d** in very good yields.

9-Methyl-6′,7-diphenyl-3,4-dihydro-1′H,2H-spiro-[acridine-1,2′-quinazolin]-4′(3′H)-one ***(6c)***. Nature: a brown powder; yield: 92%; R_f (30% EtOAc−hexane): 0.40, M.P: 250−252 °C. FTIR(KBr)ν_{max}: 3244, 3057, 2924, 1647, 1481,756 cm^{-1}; ^1H NMR (400 MHz, $CDCl_3$): δ 8.06 (s, 1H), 7.91 (s, 1H), 7.84 (t, J = 9.0 Hz, 1H), 7.80−7.72 (m, 1H), 7.54−7.41 (m, 5H), 7.41−7.24 (m, 5H), 7.25−7.14 (m, 1H), 6.71 (t, J = 10.5 Hz, 1H), 6.50 (d, J = 6.2 Hz, 1H), 5.11 (s, 1H), 3.01 (s, 2H), 2.76 (s, 3H), 2.45−2.15 (m, 2H), 1.82 (s, 2H). ^{13}C NMR (101 MHz, $CDCl_3$): δ 163.5, 157.9, 148.5, 146.1, 144.4, 140.4, 140.1, 138.83, 133.1, 131.8, 130.1, 129.2, 129.1, 128.8, 128.2, 127.8, 127.5, 127.3, 127.2, 126.8, 126.4, 121.8, 115.2, 114.2, 71.3, 39.8, 35.0, 27.5, 18.1, 16.9 HRMS-ESI: calcd for $C_{33}H_{27}N_3O$ $[M + H]^+$ m/z: 482.2232; found 482.223.

9-Methyl-6′,7-bis(3-nitrophenyl)-3,4-dihydro-1′H, 2H-spiro[acridine-1,2′-quinazolin]-4′(3′H)-one ***(6d)***. Nature: a brown powder; yield: 89%; R_f (30% EtOAc−hexane): 39, M.P: 262−263 °C. FTIR(KBr)ν_{max}: 3215, 2922, 2852, 1658, 1514, 1344, 736 cm^{-1}; ^1H NMR (400 MHz, $CDCl_3$): δ 8.26 (d, J = 9.1 Hz, 1H), 8.12−7.98 (m, 4H), 7.90 (d, J = 8.7 Hz, 1H), 7.83 (d, J = 7.6 Hz, 1H), 7.75 (d, J = 7.6 Hz, 2H), 7.59−7.49 (m, 2H), 7.46 (t, J = 8.0 Hz, 1H), 7.06 (s, 1H), 6.74 (m, 1H), 5.19 (s, 1H), 3.14 (d, J = 5.8 Hz, 2H), 2.98 (s, 3H), 2.54−2.27 (m, 2H), 1.98−1.88 (m, 2H). ^{13}C NMR (101 MHz, $CDCl_3$): δ 163.4, 158.9, 148.8, 148.7, 145.2, 142.0, 141.6, 136.3, 133.3, 133.1, 132.1, 130.0, 129.8, 129.4, 129.1, 128.3, 127.0, 122.5, 122.5, 122.1, 121.5, 120.9, 115.6, 114.2, 71.4, 40.0, 34.9, 18.1, 17.1 HRMS-ESI: calcd for $C_{33}H_{25}N_5O_5$ $[M + H]^+$ m/z: 572.1934; found 572.1924.

9-Methyl-3,4-dihydroacridin-1(2H)-one ***(5a)***. Nature: a colorless powder; R_f (15% EtOAc−hexane): 0.50, M. P: 65−66 °C. FTIR(KBr)ν_{max}: 2926, 1676, 1552, 1203, 840, 758, 696 cm^{-1}; ^1H NMR (400 MHz, $CDCl_3$): δ 8.14 (d, J = 8.5 Hz, 1H), 7.94 (d, J = 8.4 Hz, 1H), 7.70 (t, J = 7.6 Hz, 1H), 7.50 (t, J = 7.7 Hz, 1H), 3.21 (t, J = 6.3 Hz, 2H), 2.98 (s, 3H), 2.74 (t, J = 6.6 Hz, 2H), 2.28−1.97 (m, 2H). ^{13}C NMR (101 MHz, $CDCl_3$): δ 200.8,162.2, 150.1, 148.0, 131.6, 129.2, 127.8, 126.5, 125.6, 125.5, 41.2, 34.9, 21.4, 16.2.

3,3,9-Trimethyl-3,4-dihydroacridin-1(2H)-one ***(5b)***. Nature: a colorless powder; R_f (15% EtOAc−hexane): 0.60, M. P: 105−1076 °C. FTIR(KBr)ν_{max}: 2960, 1691, 1556, 1259, 1014, 763 cm^{-1}; ^1H NMR (400 MHz, $CDCl_3$): δ 8.17 (d, J = 8.6 Hz, 1H), 8.05 (d, J = 8.4 Hz, 1H), 7.74 (t, J = 7.6 Hz, 1H), 7.54 (t, J = 7.7 Hz, 1H), 3.18 (s, 2H), 3.03 (s, 3H), 2.60 (s, 2H), 1.07 (s, 6H). ^{13}C NMR (101 MHz, $CDCl_3$): δ 200.0, 160.9, 132.3, 128.9, 128.2, 127.8, 127.0, 126.2, 125.7, 124.3, 54.8, 47.7, 32.2, 28.3, 21.4, 16.3.

7-Bromo-9-methyl-3,4-dihydroacridin-1(2H)-one ***(5c)***. Nature: a colorless powder; R_f (15% EtOAc−hexane): 0.52, M. P: 83−85 °C. FTIR(KBr)ν_{max}: 3251, 1662,1558, 1375, 1172, 1076, 910, 831 cm^{-1}; ^1H NMR (400 MHz, $CDCl_3$): δ 8.09 (d, J = 1.4 Hz, 1H), 7.65 (dt, J = 8.9, 5.3 Hz, 2H), 3.11 (t, J = 6.3 Hz, 2H), 2.79 (s, 3H), 2.69 (t, J = 6.6 Hz, 2H), 2.15−2.02 (m, 2H). ^{13}C NMR (101 MHz, $CDCl_3$): δ 200.1, 162.4, 148.5, 146.3, 134.5, 130.7, 128.7, 127.63, 125.6, 120.3, 40.9, 34.6, 21.1, 15.9. HRMS-ESI: calcd for $C_{14}H_{12}BrNO$ $[M + H]^+$ m/z: 290.1433; found 290.0160.

7-Bromo-3,3,9-trimethyl-3,4-dihydroacridin-1(2H)-one ***(5d)***. Nature: a colorless powder; R_f (15% EtOAc−hexane): 0.63, M. P: 105−107 °C. FTIR(KBr)ν_{max}: 3072, 2939, 2873, 1670, 1556, 1479, 906, 827 cm^{-1}; ^1H NMR (400 MHz, $CDCl_3$): δ 8.28 (d, J = 1.9 Hz, 1H), 7.77 (m, 2H), 3.08 (s, 2H), 2.94 (s, 3H), 2.60 (s, 2H), 1.06 (s, 6H). ^{13}C NMR (101 MHz, $CDCl_3$): δ 200.5, 161.6, 148.7, 147.0, 134.8, 131.0, 129.1, 128.0, 124.8, 120.6, 54.9, 48.6, 32.2, 28.4, 16.0 HRMS-ESI: calcd for $C_{16}H_{16}BrNO$ $[M + H]^+$ m/z: 318.0493; found 318.0497.

3,9-Dimethyl-3,4-dihydroacridin-1(2H)-one ***(5e)***. Nature: a colorless powder; R_f (15% EtOAc−hexane): 0.55, M. P: 78−80 °C. FTIR(KBr)ν_{max}: 2947, 1674, 1560, 1211, 759 cm^{-1}; ^1H NMR (400 MHz, $CDCl_3$): δ 8.14 (d, J = 8.5 Hz, 1H), 7.93 (d, J = 8.4 Hz, 1H), 7.70 (t, J = 7.6 Hz, 1H), 7.49 (t, J = 7.6 Hz, 1H), 3.29 (d, J = 16.0 Hz, 1H), 2.98 (s, 3H), 2.94−2.76 (m, 2H), 2.39 (m, 2H), 1.13 (d, J = 6.1 Hz, 3H). ^{13}C NMR (101 MHz, $CDCl_3$): 200.4, 162.6, 148.9, 146.6, 134.8, 131.0, 129.1, 127.9, 125.9, 120.5, 41.1, 34.8, 21.3, 16.1.

7-Bromo-3,9-dimethyl-3,4-dihydroacridin-1(2H)-one ***(5f)***. Nature: a colorless powder; R_f (15% EtOAc−hexane): 0.56, M. P: 93−94 °C. FTIR(KBr)ν_{max}: 3572, 3452, 3319, 1656, 1558, 1219, 840 cm^{-1}; colorless powder; R_f (15% EtOAc−hexane): 0.56, M. P: 93−94 °C ^1H NMR (400 MHz, $CDCl_3$): δ 8.26 (s, 1H), 7.78 (m, 2H), 3.28 (d, J = 16.2 Hz, 1H), 3.00−2.74 (m, 5H), 2.52−2.27 (m, 2H), 1.13 (d, J = 6.2 Hz, 3H). ^{13}C NMR (101 MHz, $CDCl_3$): δ 200.3, 162.0, 149.0, 146.5, 135.0, 130.8, 129.0, 127.9, 125.3, 120.7, 49.2, 42.8, 28.5, 21.2, 16.1. HRMS-ESI: calcd for $C_{15}H_{14}BrNO$ $[M + H]^+$ m/z: 304.0337; found 304.0375.

10-Methyl-1,6,7,8-tetrahydrofuro[3,4-b]acridin-9(3H)-one ***(5g)***. Nature: a colorless powder; R_f (15% EtOAc−hexane): 0.50, M. P: 112−114 °C. FTIR(KBr)ν_{max}: 1697, 1641, 1589, 1452, 1257, 1174, 1114, 819, 715, 529 cm^{-1}; ^1H NMR (400 MHz, $CDCl_3$): δ 7.31 (s, 1H), 7.20 (s, 1H), 6.05 (s, 2H), 3.18−3.08 (m, 2H), 2.83 (s, 3H), 2.68 (t, J = 6.6 Hz, 2H), 2.09 (m, 2H). ^{13}C NMR (101 MHz, $CDCl_3$): δ 200.60, 160.63, 152.31, 148.19, 148.06, 146.99, 124.55, 124.12, 105.40, 102.18, 100.74, 41.14, 34.45, 21.59, 16.53. HRMS-ESI: calcd for $C_{15}H_{13}NO_3$ $[M + H]^+$ m/z: 256.0978; found 256.0941.

■ ASSOCIATED CONTENT

Supporting Information

The Supporting Information is available free of charge at https://pubs.acs.org/doi/10.1021/acsomega.2c00674.

https://doi.org/10.1021/acsomega.2c00674
ACS Omega 2022, 7, 20605−20618

Copies of FTIR, ^{1}H NMR,^{13}C NMR, and HRMS data for all of the new compounds and basic crystallographic data of compound **4b** (PDF)

Single-crystal XRD data for compound **4b** (CIF)

AUTHOR INFORMATION

Corresponding Authors

Shanmugam Ponnusamy − *Organic and Bioorganic Chemistry Division, CSIR-Central Leather Research Institute (CLRI), Chennai 600020, India;* orcid.org/0000-0003-0411-1982; Phone: (+91)- 44-24437130; Email: shanmu196@rediffmail.com; Fax: (+) 91-44-24911589

Kannadasan Sathananthan − *Department of Chemistry, School of Advanced Sciences, VIT, Vellore 632014, India;* orcid.org/0000-0002-5108-9303; Email: kannadasan.s@vit.ac.in

Authors

Kevin George − *Department of Chemistry, School of Advanced Sciences, VIT, Vellore 632014, India*

Pavithra Elavarasan − *Department of Chemistry, School of Advanced Sciences, VIT, Vellore 632014, India*

Complete contact information is available at: https://pubs.acs.org/10.1021/acsomega.2c00674

Funding

K.S. thanks VIT Management for providing VIT SEED GRANT for carrying out this work.

Notes

The authors declare no competing financial interest.

ACKNOWLEDGMENTS

K.G. and P.E. thank VIT, Vellore, for research fellowships. S.K. thanks VIT Management for providing infrastructure facilities for carrying out this work.

REFERENCES

(1) Kumar, S.; Bawa, S.; Gupta, H. Biological activities of quinoline derivatives. *Mini-Rev. Med. Chem.* **2009**, *9*, 1648−1654.

(2) Cho, C. S.; Oh, B. H.; Shim, S. C. Synthesis of quinolines by ruthenium-catalyzed heteroannulation of anilines with 3-amino-1-propanol. *J. Heterocycl. Chem.* **1999**, *36*, 1175−1178.

(3) Makioka, Y.; Shindo, T.; Taniguchi, Y.; Takaki, K.; Fujiwara, Y. Ytterbium (III) triflate catalyzed synthesis of quinoline derivatives from N-arylaldimines and vinyl ethers. *Synthesis* **1995**, *1995*, 801−804.

(4) Sangu, K.; Fuchibe, K.; Akiyama, T. A novel approach to 2-arylated quinolines: electrocyclization of alkynyl imines via vinylidene complexes. *Org. Lett.* **2004**, *6*, 353−355.

(5) Crousse, B.; Bégué, J. P.; Bonnet-Delpon, D. Synthesis of tetrahydroquinoline derivatives from α-CF3-N-arylaldimine and vinyl ethers. *Tetrahedron Lett.* **1998**, *39*, 5765−5768.

(6) Crousse, B.; Bégué, J. P.; Bonnet-Delpon, D. Synthesis of 2-CF (3)-tetrahydroquinoline and quinoline derivatives from CF (3)-N-aryl-aldimine. *J. Org. Chem.* **2000**, *65*, 5009−5013.

(7) Katritzky, A. R.; Arend, M. A convenient and highly regioselective one-pot synthesis of quinolines by addition of a Vilsmeier-type reagent to N-arylimines. *J. Org. Chem.* **1998**, *63*, 9989−9991.

(8) Abdelsalam, E. A.; Zaghary, W. A.; Amin, K. M.; Abou Taleb, N. A.; Mekawey, A. A.; Eldehna, W. M.; Abdel-Aziz, H. A.; Hammad, S. F. Synthesis and in vitro anticancer evaluation of some fused indazoles, quinazolines and quinolines as potential EGFR inhibitors. *Bioorg. Chem.* **2019**, *89*, No. 102985.

(9) Novanna, M.; Kannadasan, S.; Shanmugam, P. Phosphotungstic acid mediated, microwave assisted solvent-free green synthesis of highly functionalized 2'-spiro and 2, 3-dihydro quinazolinone and 2-methylamino benzamide derivatives from aryl and heteroaryl 2-amino amides. *Tetrahedron Lett.* **2019**, *60*, 201−206.

(10) Liu, X.; Fu, H.; Jiang, Y.; Zhao, Y. A Simple and Efficient Approach to Quinazolinones under Mild Copper-Catalyzed Conditions. *Angew. Chem.* **2009**, *121*, 354−357.

(11) Xu, W.; Jin, Y.; Liu, H.; Jiang, Y.; Fu, A. H. Copper-Catalyzed Domino Synthesis of Quinazolinones via Ullmann-Type Coupling and Aerobic Oxidative C− H Amidation. *Org. Lett.* **2011**, *13*, 1274−1277.

(12) Zhou, J.; Fang, J. One-pot synthesis of quinazolinones via iridium-catalyzed hydrogen transfers. *J. Org. Chem.* **2011**, *76*, 7730−7736.

(13) Zhang, Z.; Wang, M.; Zhang, C.; Zhang, Z.; Lu, J.; Wang, F. The cascade synthesis of quinazolinones and quinazolines using an α-MnO_2 catalyst and tert-butyl hydroperoxide (TBHP) as an oxidant. *Chem. Commun.* **2015**, *51*, 9205−9207.

(14) Zheng, J.; Zhang, Y.; Wang, D.; Cui, S. Silver (I)-Mediated Phosphorylation/Cyclization Cascade of N-Cyanamide Alkenes for Divergent Access to Quinazolinones and Dihydroisoquinolinones. *Org. Lett.* **2016**, *18*, 1768−1771.

(15) Bie, Z.; Li, G.; Wang, L.; Lv, Y.; Niu, J.; Gao, S. A facile vanadium-catalyzed aerobic oxidative synthesis of quinazolinones from 2-aminobenzamides with aldehydes or alcohols. *Tetrahedron Lett.* **2016**, *57*, 4935−4938.

(16) Sharma, M.; Pandey, S.; Chauhan, K.; Sharma, D.; Kumar, B.; Chauhan, P. M. Cyanuric chloride catalyzed mild protocol for synthesis of biologically active dihydro/spiro quinazolinones and quinazolinone-glycoconjugates. *J. Org. Chem.* **2012**, *77*, 929−937.

(17) Rambabu, D.; Kumar, S. K.; Sreenivas, B. Y.; Sandra, S.; Kandale, A.; Misra, P.; Rao, M. B.; Pal, M. Ultrasound-based approach to spiro-2, 3-dihydroquinazolin-4 (1H)-ones: their in vitro evaluation against chorismate mutase. *Tetrahedron Lett.* **2013**, *54*, 495−501.

(18) Salehi, P.; Dabiri, M.; Baghbanzadeh, M.; Bahramnejad, M. One-Pot, Three-Component Synthesis of 2, 3-Dihydro-4 (1 H)-quinazolinones by Montmorillonite K-10 as an Efficient and Reusable Catalyst. *Synth. Commun.* **2006**, *36*, 2287−2292.

(19) Revathy, K.; Lalitha, A. p-TSA-catalyzed synthesis of spiroquinazolinones. *J. Iran. Chem. Soc.* **2015**, *12*, 2045−2049.

(20) Shaterian, H. R.; Rigi, F. An efficient synthesis of quinazoline and xanthene derivatives using starch sulfate as a biodegradable solid acid catalyst. *Res. Chem. Intermed.* **2015**, *41*, 721−738.

(21) Yang, X.; Cheng, G.; Shen, J.; Kuai, C.; Cui, X. Cleavage of the C−C triple bond of ketoalkynes: synthesis of 4 (3 H)-quinazolinones. *Org. Chem. Front.* **2015**, *2*, 366−368.

(22) (a) Venkateshwarlu, R.; Murthy, V. N.; Tadiparthi, K.; Nikumbh, S. P.; Jinkala, R.; Siddaiah, V.; Madhu babu, M. V.; Mohan, H. R.; Raghunadh, A. Base mediated spirocyclization of quinazoline: one-step synthesis of spiro-isoindolinone dihydroquinazolinones. *RSC Adv.* **2020**, *10*, 9486−9491. (b) Sharma, M.; Pandey, S.; Chauhan, K.; Sharma, D.; Kumar, B.; Chauhan, P. M. Cyanuric chloride catalyzed mild protocol for synthesis of biologically active dihydro/spiro quinazolinones and quinazolinone-glycoconjugates. *J. Org. Chem.* **2012**, *77*, 929−937.

(23) (a) Auti, P. S.; George, G.; Paul, A. T. Recent advances in the pharmacological diversification of quinazoline/quinazolinone hybrids. *RSC Adv.* **2020**, *10*, 41353−41392. (b) Han, S.; Sang, Y.; Wu, Y.; Tao, Y.; Pannecouque, C.; De Clercq, E.; Zhuang, C.; Chen, F. E. Molecular hybridization-inspired optimization of diarylbenzopyrimidines as HIV-1 nonnucleoside reverse transcriptase inhibitors with improved activity against K103N and E138K mutants and pharmacokinetic profiles. *ACS Infect. Dis.* **2020**, *6*, 787−801.

(24) Cagir, A.; Jones, S. H.; Gao, R.; Eisenhauer, B. M.; Hecht, S. M. Luotonin A. A naturally occurring human DNA topoisomerase I poison. *J. Am. Chem. Soc.* **2003**, *125*, 13628−13629.

(25) Broadwater, S. J.; Roth, S. L.; Price, K. E.; Kobašlija, M.; McQuade, D. T. One-pot multi-step synthesis: a challenge spawning innovation. *Org. Biomol. Chem.* **2005**, *3*, 2899−2906.
(26) Kwon, S. H.; Seo, H. A.; Cheon, C. H. Total synthesis of luotonin A and rutaecarpine from an aldimine via the designed cyclization. *Org. Lett.* **2016**, *18*, 5280−5283.
(27) Badolato, M.; Aiello, F.; Neamati, N. 2, 3-Dihydroquinazolin-4 (1 H)-one as a privileged scaffold in drug design. *RSC Adv.* **2018**, *8*, 20894−20921.
(28) CCDC-2101995(compound 4b) contains the supplementary crystallographic data for this paper.This data can be obtained free of charge from the Cambridge CrystallographicData Centre via. www.ccdc.cam.ac.uk/datarequest/cif
(29) Nigam, S.; Rutan, S. Principles and applications of solvatochromism. *Appl. Spectrosc.* **2001**, *55*, 362A−370A.
(30) Allaoui, Z. I. M.; Le Gall, E.; Fihey, A.; Plaza-Pedroche, R.; Katan, C.; Robin-Le Guen, F.; Rodriguez-Lopez, J.; Achelle, S. Push-pull (iso) quinoline chromophores: synthesis, photophysical properties, and use for white light emission. *Chem. - Eur. J.* **2020**, *26*, 8153−8161.
(31) Novanna, M.; Kannadasan, S.; Shanmugam, P. Microwave assisted synthesis and photophysical properties of blue emissive 2-amino-3-carboxamide-1, 1′-biaryls and 4-(arylamino)-[1, 1′-biphenyl]-3-carboxamides via Suzuki and Chan-Evans-Lam coupling. *Dyes. Pigm.* **2020**, *174*, 108015−108024.
(32) Pillai, S.; Kozlov, M.; Marras, S. A.; Krasnoperov, L. N.; Mustaev, A. New cross-linking quinoline and quinolone derivatives for sensitive fluorescent labeling. *J. Fluoresc.* **2012**, *22*, 1021−1032.
(33) Mamidala, R.; Subramani, M. S.; Samser, S.; Biswal, P.; Venkatasubbaiah, K. Chemoselective Alkylation of Aminoacetophenones with Alcohols by Using a Palladacycle-Phosphine Catalyst. *Eur. J. Org. Chem* **2018**, *2018*, 6286−6296.
(34) Laha, J. K.; Manral, N.; Hunjan, M. K. Palladium-catalysed regioselective N-arylation of anthranilamides: a tandem route for dibenzodiazepinone synthesis. *New. J. Chem* **2019**, *43*, 7339−7343.
(35) Rahmannejadi, N.; Yavari, I.; Khabnadideh, S. Synthesis and antitumor activities of novel bis-quinazolin-4 (3H)-ones. *J. Heterocycl. Chem.* **2020**, *57*, 978−982.

https://doi.org/10.1021/acsomega.2c00674
ACS Omega 2022, 7, 20605−20618